Forest Ecology and Management 259 (2010) 1311–1327

Contents lists available at ScienceDirect

Forest Ecology and Management

journal homepage: www.elsevier.com/locate/foreco

Model estimates of net primary productivity, evapotranspiration, and water use efficiency in the terrestrial ecosystems of the southern United States during 1895–2007

Hanqin Tian [a,*], Guangsheng Chen [a], Mingliang Liu [a], Chi Zhang [a], Ge Sun [b], Chaoqun Lu [a], Xiaofeng Xu [a], Wei Ren [a], Shufen Pan [a], Arthur Chappelka [a]

[a] Ecosystem Dynamics and Global Ecology Laboratory, School of Forestry and Wildlife Sciences, Auburn University, Auburn, AL 36849, USA
[b] Southern Global Change Program, USDA Forest Service, 920 Main Campus Drive, Raleigh, NC 27606, USA

ARTICLE INFO

Article history:
Received 17 May 2009
Received in revised form 3 October 2009
Accepted 12 October 2009

Keywords:
Net primary productivity (NPP)
Evapotranspiration (ET)
Dynamic Land Ecosystem Model (DLEM)
Water use efficiency (WUE)
Southern United States

ABSTRACT

The effects of global change on ecosystem productivity and water resources in the southern United States (SUS), a traditionally 'water-rich' region and the 'timber basket' of the country, are not well quantified. We carried out several simulation experiments to quantify ecosystem net primary productivity (NPP), evapotranspiration (ET) and water use efficiency (WUE) (i.e., NPP/ET) in the SUS by employing an integrated process-based ecosystem model (Dynamic Land Ecosystem Model, DLEM). The results indicated that the average ET in the SUS was 710 mm during 1895–2007. As a whole, the annual ET increased and decreased slightly during the first and second half of the study period, respectively. The mean regional total NPP was 1.18 Pg C/yr (525.2 g C/m^2/yr) during 1895–2007. NPP increased consistently from 1895 to 2007 with a rate of 2.5 Tg C/yr or 1.10 g C/m^2/yr, representing a 27% increase. The average WUE was about 0.71 g C/kg H_2O and increased about 25% from 1895 to 2007. The rather stable ET might explain the resulting increase in WUE. The average WUE of different biomes followed an order of: forest (0.93 g C/kg H_2O) > wetland (0.75 g C/kg H_2O) > grassland (0.58 g C/kg H_2O) > cropland (0.54 g C/kg H_2O) > shrubland (0.45 g C/kg H_2O). WUE of cropland increased the fastest (by 30%), followed by shrubland (17%) and grassland (9%), while WUE of forest and wetland changed little from the period of 1895–1950 to the period of 1951–2007. NPP, ET and WUE showed substantial inter-annual and spatial variability, which was induced by the non-uniform distribution patterns and change rates of environmental factors across the SUS. We concluded that an accurate projection of the regional impact of climate change on carbon and water resources must consider the spatial variability of ecosystem water use efficiency across biomes as well as the interactions among all stresses, especially land-use and land-cover change and climate.

1. Introduction

Ecosystem productivity and water use (i.e., evapotranspiration, ET) are tightly coupled at multiple scales (Chapin et al., 2002; Waring and Running, 2007). In terrestrial ecosystems, for example, water availability is the primary limiting factor for plant growth in over 40% of vegetated areas, while another 33% of the area is limited by cold temperatures and frozen water, where the water is not available for plant growth (Nemani et al., 2003). Vegetation can respond to water stress in several ways: increasing water uptake from soil, increasing water use efficiency (WUE) and reducing water losses, etc. (Hsiao, 1973; Waring and Running, 2007). Determining the functional responses of plants to water stress is still one of the most complex issues in plant stress biology (Bray, 1997). In order to respond to global environmental change with sound land management practices, there must be a clear understanding of how multiple stresses affect all ecosystem processes.

It is likely that global climate changes will continue to influence the Northern Hemisphere's precipitation distributions, with increased frequency, duration and intensity of drought and other extreme climate events (Saxe et al., 2001; IPCC, 2001, 2007; Salinger et al., 2005). These changes imply that in the future, water distribution among different terrestrial ecosystems will be more variable. In the mean time, changes in other factors such as land-use and land-cover types and atmospheric composition (tropospheric ozone, atmospheric CO_2 and nitrogen deposition) interact

* Corresponding author. Tel.: +1 334 844 1059; fax: +1 334 844 1084.
E-mail address: tianhan@auburn.edu (H. Tian).

0378-1127/$ – see front matter © 2009 Elsevier B.V. All rights reserved.
doi:10.1016/j.foreco.2009.10.009

with global climate change to influence the water budget, plant water use strategy, and the global carbon cycle. Understanding the interactions between the carbon and water cycles has been recognized as one of the gaps in global change research (Jackson et al., 2005; Ehleringer et al., 2000; Pereira et al., 2004).

There are many methods of addressing the interactions between the water and carbon cycles. Of these, WUE, the ratio of carbon gain during plant photosynthesis to water loss during evapotranspiration, is an essential concept for studying these interactive effects because it couples the water and carbon cycles very well. WUE can also be defined in various ways at different spatial scales or for different study objectives (Hsiao, 1973; de Wit, 1958; Farquhar and Sharkey, 1982; Donovan and Ehleringer, 1991; Jones, 1992; Steduto, 1996). Field measurements of WUE for few ecosystems have become available (e.g., Law et al., 2002; Yu et al., 2008; Sun et al., 2002) in recent decades thanks to the development of eddy covariance systems. However, due to complex interactions between water and carbon and uncertainty in the interactive influences of multiple environmental factors on WUE in a large-scale ecosystem, the long-term dynamics of WUE on a large scale have rarely been quantified. The emergence and application of mechanism-based models have made it possible to scale up WUE from stand or field level to ecosystem level and to better understand the impact of individual and multiple environmental factors on WUE.

The southern United States (SUS) has experienced significant changes in climate, atmospheric composition, and land-use and land-cover types during the 20th century (IPCC, 2007; Schimel et al., 2000; Norby et al., 2005; Chappelka and Samuelson, 1998; Felzer et al., 2004; Holland et al., 2005; Dentener, 2006; Chen et al., 2006a; Woodbury et al., 2007; Birdsey et al., 2006). The SUS has relatively higher forest coverage, is one of the major suppliers of wood products and has some of the greatest potential for carbon sequestration in the country (Birdsey and Heath, 1995; Birdsey and Lewis, 2003; Woodbury et al., 2007). However, there are increasing concerns about rapid urbanization, wetland losses, extreme climatic conditions (such as severe droughts and floods), and forest plantation expansion and how these are impacting regional water and carbon resources (Sun et al., 2008; McNulty et al., 1997; Jackson et al., 2005). We are not aware of much work that has been done to quantify the long-term dynamics of ecosystem water use and its interactions with ecosystem productivity in the SUS.

This study used a well-evaluated integrated ecosystem model (Dynamic Land Ecosystem Model, DLEM) and constructed long-term data of environmental factors to simulate the spatial and temporal changes of water, nitrogen and carbon cycles. Our objectives were to quantify: (1) Ecosystem NPP, ET and WUE in the southern United States; (2) Impacts of changing environmental factors (combined changes in climate, land-use and land-cover types, atmospheric CO_2 concentration, nitrogen deposition, and tropospheric ozone concentration) on the NPP, ET and WUE of different ecosystems.

2. Methodology

2.1. Ecosystem water use efficiency calculation

Water use efficiency can be defined in many ways. On an ecosystem scale, three major definitions are generally used: (1) Gross primary production (GPP) based WUE: GPP/ET; (2) Net primary productivity (NPP) based WUE: NPP/ET; (3) Net ecosystem carbon production (NEP) based WUE: NEP/ET. Annual rainfall was also used to replace ET to calculate rainfall use efficiency (RUE, e.g., Huxman et al., 2004; Bai et al., 2008). In this study, we primarily used the second definition (NPP-based WUE) to address the objectives since NPP could reflect annual net carbon fixation in the plant biomass. The other two calculation methods were used to compare our results with those of previous studies. Ecosystem WUE for an individual grid cell was calculated as annual NPP in the grid cell divided by annual ET. The mean WUE over a region, a biome or a treatment was calculated as the area-weighted average value of all grid cells. The WUE of cropland was calculated in the same way as non-irrigated cropland and natural vegetation types in this study.

2.2. Model description

The Dynamic Land Ecosystem Model (DLEM) is a highly integrated process-based terrestrial ecosystem model that simulates daily carbon, water and nitrogen cycles driven by the changes in atmospheric chemistry including ozone, nitrogen deposition, CO_2 concentration, climate, land-use and land-cover types and disturbances (i.e., fire, hurricane, and harvest) (Fig. 1). The DLEM is well documented and well evaluated and has been extensively used in studying the terrestrial carbon, water and nitrogen cycles over Monsoon Asia, the continental U.S., and South America (e.g., Tian et al., 2005, 2008, submitted for publication; Chen et al., 2006b; Ren et al., 2007a,b; Liu et al., 2007, 2008; Zhang et al., 2007).

DLEM includes four core components (Fig. 1): (1) biophysics, (2) plant physiology, (3) soil biogeochemistry, and (4) dynamic vegetation and land-use. The biophysical component includes the instantaneous exchanges of energy, water, and momentum with the atmosphere, which involves micrometeorology, canopy structure, soil physics, radiative transfer, water and energy flow, and momentum movement. The plant physiology component in DLEM simulates major physiological processes such as photosynthesis, respiration, carbohydrate allocation among various organs (root, stem and leaf), nitrogen uptake, transpiration, phenology, etc. The component of soil biogeochemistry simulates mineralization, nitrification/denitrification, decomposition and fermentation so that DLEM is able to estimate simultaneous emission of multiple trace gases (CO_2, CH_4 and N_2O). The dynamic vegetation component simulates two kinds of processes: the biogeography redistribution of plant functional types under environmental changes, and plant competition and succession during vegetation recovery after disturbances. Like most Dynamic Global Vegetation Models (DGVMs), DLEM builds on the concept of plant functional types (PFT) to describe vegetation distributions. The DLEM has also emphasized water, carbon and nitrogen cycles in managed ecosystems such as cropland, forest plantation, and pasture. The key processes for modeling GPP, NPP, and ET in DLEM are briefly described below.

GPP simulation: A modified Farquar's model is used to simulate gross primary production in DLEM (Farquhar et al., 1980; Collatz et al., 1991, 1992; Dougherty et al., 1994; Bonan, 1996; Sellers et al., 1996). The canopy is divided into sunlit and shaded layers. GPP ($g\,C/m^2/day$) is calculated by scaling leaf assimilation rates ($\mu mol\,CO_2\,m^{-2}\,s^{-1}$) up to the whole canopy:

$$GPP_{sun} = 12.01 \times 10^{-6} \times A_{sun} \times plai_{sun} \times day1 \times 3600$$

$$GPP_{shade} = 12.01 \times 10^{-6} \times A_{shade} \times plai_{shade} \times day1 \times 3600$$

$$GPP = GPP_{sun} + GPP_{shade}$$

where GPP_{sun} and GPP_{shade} are gross primary productivity of sunlit and shaded canopy, respectively; A_{sun} and A_{shade} are assimilation rates of sunlit and shaded canopy; $plai_{sun}$ and $plai_{shade}$ are the sunlit and shaded leaf area indices; dayl is daytime length (s) in a day. 12.01×10^{-6} is a constant to change the unit from $\mu mol\,CO_2$ to gram C.

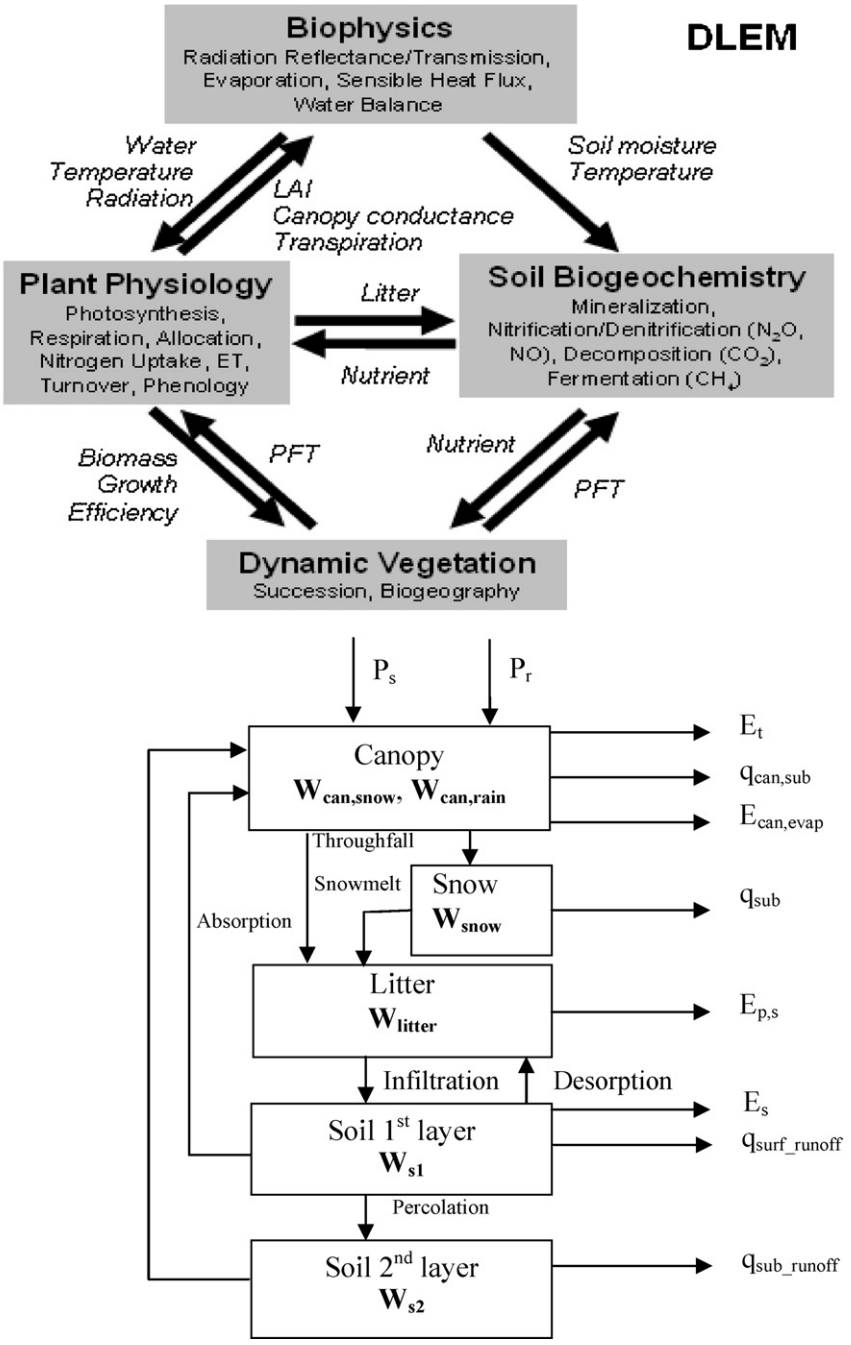

Fig. 1. Framework of the Dynamic Land Ecosystem Model (DLEM, top one) and the hydrological component in DLEM (below one). *Note*: The soil is represented by three layers: a litter layer (or above surface water) with varied depth, and two mineral soil layers with fixed depths of 0.5 m (0–50 cm) and 1.0 m (50–150 cm), respectively. Snow (P_s) and rain (P_r) are separated from precipitation. Canopy intercepts some of P_s and P_r into canopy snow storage ($W_{can,snow}$) and rain storage ($W_{can,rain}$), respectively. The intercepted water is eventually evaporated ($E_{can,evap}$) or sublimated ($q_{can,sub}$) to the air. The remaining P_s and P_r enter into the ground snowpack (W_{snow}) and litter layer (W_{litter}) as throughfall. The W_{litter} is over maximum water storage of the litter, extra water will be infiltrated into the first soil layer. Simultaneously, the litter layer will absorb water from the first soil layer. The water holding by the litter will be evaporated to air ($E_{p,s}$). When the soil moisture in first mineral layer (W_{s1}) exceeds the saturated soil water content, the extra water will run off from this layer which forms surface runoff ($q_{surf,runoff}$) or infiltrate in the second soil layer (W_{s2}). The water in the first soil layer will be evaporated into air (E_s). The water percolation from the second soil layer forms subsurface runoff ($q_{surf,runoff}$).

The plai_{sun} and $\text{plai}_{\text{shade}}$ are estimated as:

$$\text{plai}_{\text{sun}} = 1 - \text{EXP}(-\text{proj\_LAI})$$

$$\text{plai}_{\text{shade}} = \text{proj\_LAI} - \text{plai}_{\text{sun}}$$

where proj_LAI is the projected leaf area index.

Using similar methods to Collatz et al. (1991), DLEM determines the C assimilation rate as the minimum of three limiting rates, w_c, w_j, w_e, which represents the assimilation rates as limited by the efficiency of the photosynthetic enzymes system (Rubisco-limited), the amount of PAR captured by the leaf chlorophyll (light-limited), and the capacity of the leaf to export or utilize the products of photosynthesis products (export-limited) for C_3 species, respectively. For C_4 species, w_e refers to the PEP carboxylase-limited rate of carboxylation. The canopy sunlit and shaded carbon assimilation rate can be estimated as:

$$A = \min(w_c, w_j, w_e) \times \text{Index}_{\text{gs}}$$

where A is canopy carbon assimilation rate ($\mu\text{mol CO}_2\ \text{m}^{-2}\ \text{s}^{-1}$); w_c is assimilation rate limited by Rubisco (carboxylase-oxygenase

enzyme) (μmol CO_2 m^{-2} s^{-1}); w_j is assimilation rate limited by available light (PAR) (μmol CO_2 m^{-2} s^{-1}); w_e is assimilation rate limited by transport of photosynthetic products (C_3 species), or PEP carboxylase (C_4 species) (μmol CO_2 m^{-2} s^{-1}); $Index_{gs}$ is an indicator of growing status, which is 0 when the air temperature is less than the minimum photosynthesis temperature (no growth), and 1 when it is otherwise.

Ozone effects on GPP: DLEM uses a scalar to modify the GPP of sunlit and shaded leaves to account for the ozone impacts on GPP. It is assumed that ozone effects are accumulative on plant production. We used an empirical equation derived from several research reports (Martin et al., 2001; Ollinger et al., 1997; Felzer et al., 2004), to describe ozone limitation related to stomatal conductance and ozone concentration, as well as the accumulation of damage resulting from increasing ozone concentration in the previous time period (Ren et al., 2007a,b).

$$O_{eff}(i) = 1 - ((1 - 1/N_{day}) \times O_{eff}(i-1) + \alpha \times AOT40(i) \times g_s(i))$$

where $O_{eff}(i)$ and $O_{eff}(i-1)$ are the ozone damage to GPP at day i and $i-1$, respectively; N_{day} is the day number during the study period; α is a plant functional type specific parameter, representing the PFT's sensitivity to ozone stress; AOT40(i) is ozone accumulation (ppb) above 40 ppb at day i; $g_s(i)$ is the stomatal conductance at day i.

Ozone effects are calculated with the stomatal conductance parameters specific to sunlit and shaded leaves. When scaled up to the canopy, the leaf assimilation rate is proportionally reduced due to ozone effects.

NPP simulation: NPP is the net carbon gain by vegetation and equals the difference between GPP and plant respiration (Chapin et al., 2002). DLEM estimates maintenance respiration (Mr, unit: g C/m^2/day) and growth respiration (Gr, unit: g C/m^2/day), respectively. Gr is calculated by assuming that the fixed part of assimilated C will be used to construct new tissue (for turnover or plant growth). During these processes, 25% of assimilated C is supposed to be used as growth respiration. NPP is thus calculated as:

$$Gr = 0.25 \times GPP$$

$$NPP = GPP - Mr - Gr$$

Maintenance respiration is related to surface temperature and biomass nitrogen content. The following equation is used to calculate the maintenance respiration of leaf, sapwood, fine root, and coarse root:

$$Mr_i = rf \times R_{coeff} \times N_i \times f(T)$$

where i denotes the carbon pool of different plants (leaf, sapwood, fine root, or coarse root); Mr_i (g C/m^2/day) is the maintenance respiration of different pools; rf is a parameter indicating growing phase, which is set at 0.5 for non-growing season and 1.0 for growing season; R_{coeff} is a plant functional type specific respiration coefficient; N_i (g N m^{-2}) is the nitrogen content of pool i; $f(T)$ is the temperature factor, calculated as:

$$f(T) = e^{308.56 \times (1/56.02 - 1/(T+46.02))}$$

where T is the daily average air temperature for modeling aboveground carbon pools such as leaf, sapwood, and heartwood or soil temperature for modeling belowground pools such as coarse root and fine root.

The major hydrological processes in DLEM are shown in Fig. 1: The evapotranspiration process in DLEM includes four major components: (1) Canopy transpiration; (2) Canopy evaporation; (3) Soil evaporation; (4) Canopy snow sublimation.

Canopy ET: The canopy is divided into wet fraction and dry fraction according to Dickinson et al. (1991).

$$f_{can,wet} = \left[\frac{W_{can,rain}}{W_{can,max}}\right]^{2/3} \leq 1$$

where $f_{can,wet}$ is the wet fraction of the canopy. $W_{can,rain}$ and $W_{can,max}$ are total rainfall intercepted by canopy and the maximum canopy water holding capacity, respectively. The canopy intercepted water is estimated the same way as Bonan (1996).

Evaporation from wet surfaces is assumed to occur at the potential rate (Wigmosta et al., 1994). Transpiration from dry surfaces of vegetation is calculated using a Penman-Monteith approach (Wigmosta et al., 1994).

$$E_t = \frac{\Delta \times R_{sw,abs} + \rho \times c_p \times (e_s - e)/r_a}{\lambda \times [\Delta + \gamma \times (1 + r_c/r_a)}$$

where E_t is the rate of water transpired (mm M^{-2} s^{-1}), Δ is the slope of saturated vapor pressure–temperature curve, $R_{sw,abs}$ is the net shortwave radiation density, ρ is the density of moist air, c_p is the specific heat of air at constant pressure, e_s is the saturation vapor pressure, e is the vapor pressure, r_a is the aerodynamic resistance to vapor transport, λ is the latent heat of vaporization of water, γ is the Psychrometric constant, and r_c is the canopy resistance to vapor transport.

The potential evaporation from wet surfaces can be estimated by setting r_c equal to zero (Wigmosta et al., 1994),

$$E_p = \frac{\Delta \times R_{sw,abs} + \rho \times c_p \times (e_s - e)/r_a}{\lambda \times [\Delta + \gamma]}$$

The model calculates evaporation and transpiration independently for wet and dry surfaces. If all intercepted water is evaporated during daytime, then the wet surfaces change to dry surfaces and transpiration occurs for the remaining daytime.

$$E_{can,ep} = \min(W_{can,rain}, f_{wet} \times E_p \times t_{sub-left})$$

$$t_{pep-left} = \begin{cases} 1 - \dfrac{E_{can,ep}}{f_{wet} \times E_p \times t_{sub-left}} \times t_{sub-left} & if \quad W_{can,rain} < f_{wet} \times E_p \times t_{sub-left} \\ 0 & if \quad W_{can,rain} < f_{wet} \times E_p \times t_{sub-left} \end{cases}$$

$$E_{can,day} = E_{can,ep} + \min(AWC_s, (1 - f_{wet}) \times E_t \times t_{sub-left} + f_{wet} \times E_t \times t_{pep-left})$$

where $E_{can,evap}$ is the daily evaporation from wet surfaces; $t_{sub\text{-}left}$ is the time left after snow sublimation in a day; $t_{pevap\text{-}left}$ is the day time length after the canopy intercepted rain is evaporated, $E_{can,day}$ is the daily total canopy evapotranspiration (kg m^{-2}); $W_{can,rain}$ is the canopy intercepted rain storage (mm); AWC_s (mm) is the total available water from all soil layers except the litter layer.

Soil surface evaporation: Soil surface evaporation is influenced both by energy, atmospheric drivers and a maximum infiltration rate as a function of soil properties at a given soil moisture (Philip, 1957; Wigmosta et al., 1994). When soil is wet, a soil may be able to provide water to the surface at a rate equal to or greater than the potential evaporation demand. This condition is termed climate-controlled (Eagleson, 1978). As soil moisture is depleted, the rate of delivery falls below the potential evaporation rate and this condition is termed soil-controlled (Wigmosta et al., 1994). Using this approach, Wigmosta et al. (1994) and Entekhabi and Eagleson (1989) revised soil water evaporation (E_s).

$$E_s = (1 - f_{snow}) \times \min(E_{p,s}, F_e, W_{litter} + W_{ap})$$

$$F_e = S_e \Delta t^{1/2}$$

$$S_e = \left[\frac{8\phi K(\theta_s)\psi_b}{3(1+3m)(1+4m)}\right]^{1/2} \left[\frac{\theta}{\phi}\right]^{(1/2m)+2}$$

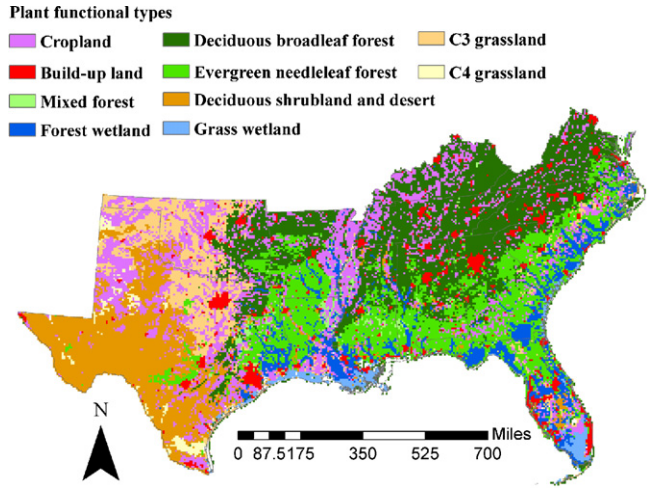

Fig. 2. The state boundary and major plant functional types in the southern United States.

where $E_{p,s}$ is the simulated soil potential evaporation; F_e is the desorption volume; S_e is the soil sorptivity; W_{avevap} is the available soil water that can be evaporated. We assume that surface evaporation can only affect the top soil layer to a depth of 50 cm, and that minimum water content after evaporation approaches at wilting point (with soil metric potential of −1500 kPa) in the 5–50 cm soil layer and zero in the top 5 cm of soil (Agam et al., 2004; Wythers et al., 1999); Φ is porosity of the soil; $K(\theta_s)$ is saturated hydraulic conductivity (mm/h); Ψ_b is air entry (bubbling) pressure (mm water); m is the pore size index; θ is the relative soil moisture; if the water table is higher than the soil surface (e.g., wetland and paddy land), E_s is equal to $E_{p,s}$; Δt is the time step of evaporation (h).

2.3. Data description

The model input data include annual historical land-use and land-cover maps, daily climate data, annual atmospheric CO_2 and daily tropospheric ozone concentrations, annual nitrogen deposition, annual N fertilizer amounts in cropland, and non-step soil property and topography data. Geospatial data were scaled to the same spatial scale (8 km × 8 km) to drive the DLEM model.

Vegetation map: A natural vegetation distribution map was generated based on multiple data sources. The base vegetation

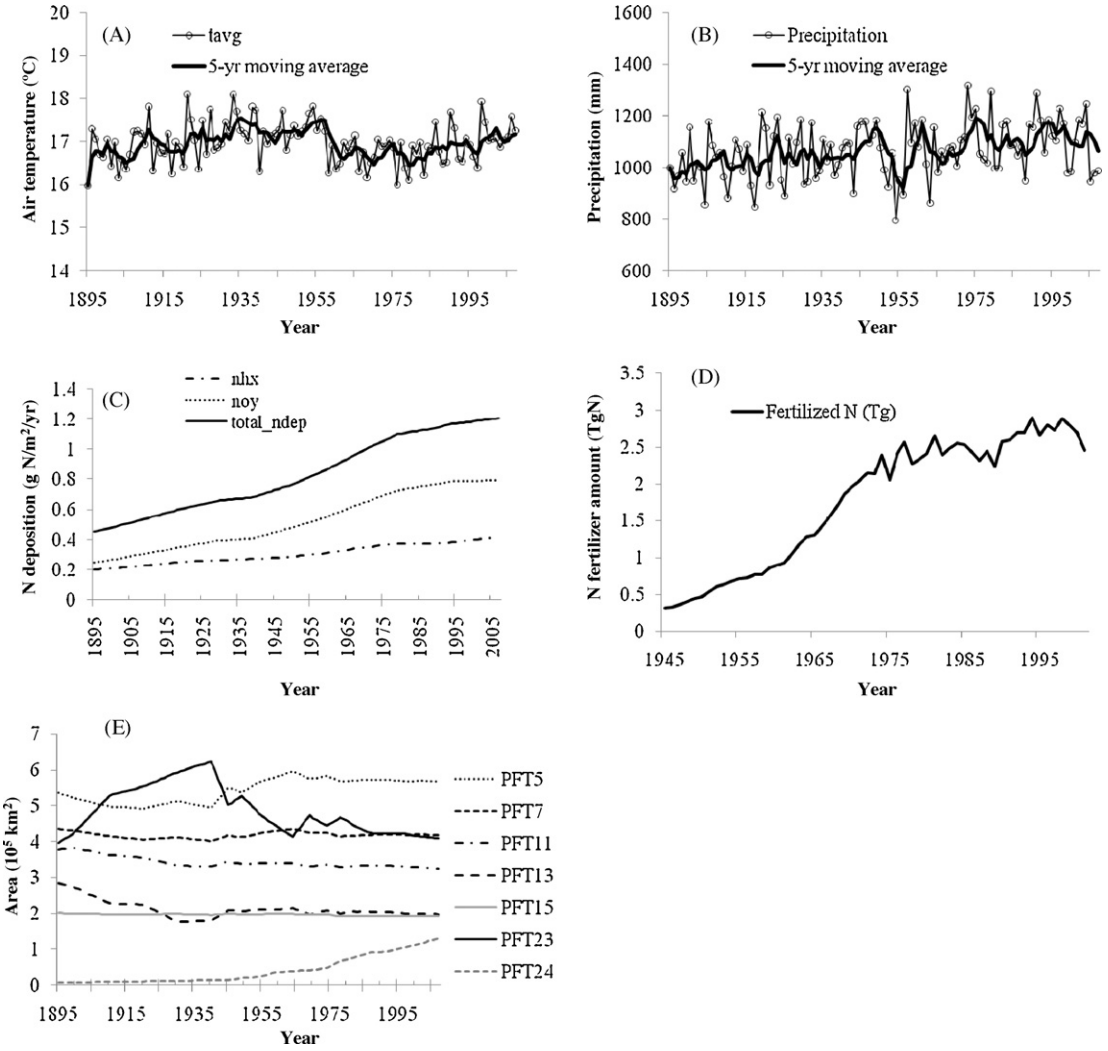

Fig. 3. Magnitude of changes in multiple environmental factors in the southern United States. *Note*: nhx, deposited nitrogen as the form of NH_x-N including NH_3 and NH_4^+-N; noy: deposited nitrogen as the form of NO_y-N including all oxidized forms of nitrogen except N_2O. (A) Mean annual temperature (°C) from 1895 to 2007; (B) annual precipitation (mm) from 1895 to 2007; (C) N deposition rate (g N/m²/yr) from 1895 to 2007; (D) N fertilizer amounts (Tg N) in the cropland from 1945 to 2001; (E) area of different biomes from 1895 to 2007 (PFT5: temperate deciduous broadleaf forest; PFT7: temperate evergreen needleleaf forest (including mixed forest); PFT11: deciduous shrubland; PFT13: C_3 and C_4 grassland; PFT15: grass and forest wetland; PFT23: cropland; PFT24: build-up land).

distribution map was from the National Land Cover Data (NLCD, 2001; Homer et al., 2004, 2007) at a resolution of 30 m. Then we used the global C_4 grassland percentage map developed by Still et al. (2003) to determine the distribution of C_4 grassland in the study region. Finally, we identified the wetland area based on the Global Lakes and Wetlands Database (GLWD) developed by Lehner and Döll (2004). We reclassified the potential vegetation types into 8 general natural plant functional groups (deciduous broadleaf forest, coniferous broadleaf forest, mixed broadleaf and coniferous forest, arid shrubland, C_3 grassland, C_4 grassland, grass wetland, and forest wetland; Fig. 2). All of these input maps were aggregated into 8 km × 8 km resolution.

Historical land-use data: Approaches similar to those of Chen et al. (2006a) and Zhang et al. (2007) were used to combine the contemporary land-use and land-cover map (which was derived from NLCD, 2001 with the historical census datasets of cropland and urban area), with population to reconstruct annual distribution maps of cropland and urban/developed lands at 8 km × 8 km resolution from 1895 to 2007.

State-level urban area data for 1945–1997 were obtained from the U.S. Census Bureau (www.census.gov). For years before 1945, we assumed that changes in urban area were positively correlated with the annual changes in population density which is available from Waisanen and Bliss (2002). For years after 1997, we assumed

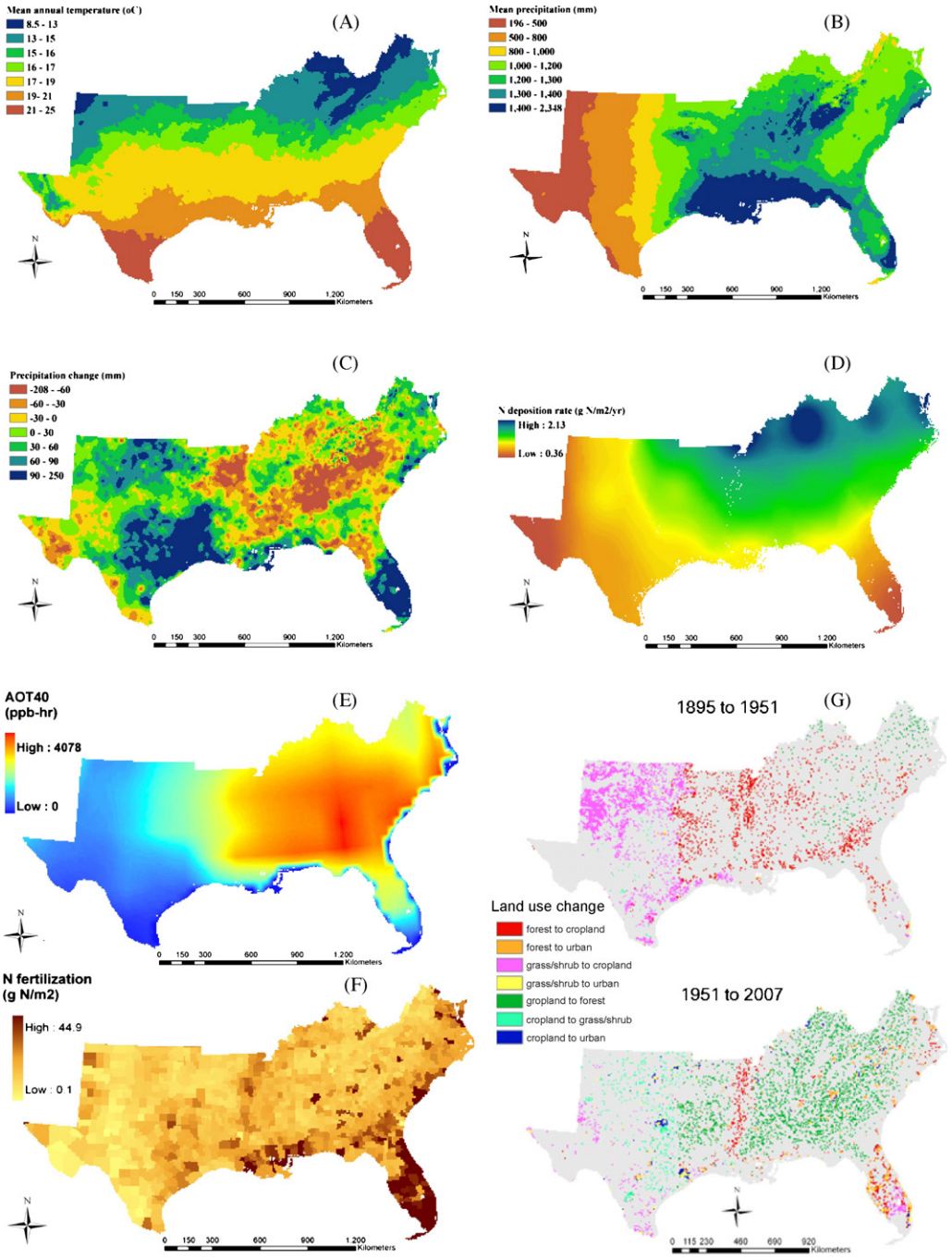

Fig. 4. Spatial pattern of environmental factors that controlled the ecological processes of the southern United States. (A) Mean annual temperature (°C) during 1895–2007; (B) Mean precipitation (mm) during 1895–2007; (C) Precipitation change (mm) from 1961–1990 to 1991–2007; (D) Nitrogen deposition rate in 2007 (g N/m^2/yr); (E) Accumulated tropospheric ozone concentration as measured by AOT40 index (ppb h) in the 1990s; (F) Annual nitrogen fertilization rate (g N/m^2/yr) in cropland in 2000; (G) Land-use change from 1895 to 1951 and from 1951 to 2007.

that the state-level urbanization rate (the ratio of the annual increased urban area to the total urban area in 1997) remained unchanged over time. We derived the annual urbanization rate of each state after 1997 by comparing 1997 and 2003 state-level urban area as reported by the USDA Natural Resources Conservation Service's web site: http://www.nrcs.usda.gov/technical/NRI/. The cropland datasets were reconstructed in the same way. The county-level cropland census data compiled by Waisanen and Bliss (2002) was used to control the annual cropland area. These census data covered the period from 1790 to 1997. The cropland distribution data from 1997 to 2003 were generated using the same methods for urban distribution. Due to the lack of a recent land-use change dataset, we assumed no land-use changes took place in the study region from 2003 to 2007.

Nitrogen fertilization dataset: Alexander and Smith (1990) and Ruddy et al. (2006) developed county-level nitrogen fertilization tabular datasets for the conterminous U.S. from 1945 to 1985 and from 1987 to 2001, respectively. By assuming the nitrogen fertilization rate of 1986 to be the average of 1985 and 1987, we combined the two datasets together and derived a county-level nitrogen fertilizer tabular dataset from 1945 to 2001. Based on the county-level cropland area census data (Waisanen and Bliss, 2002), we then derived spatial maps of nitrogen fertilization application ($g\ N\ m^{-2}$ of cropland) for the SUS from 1945 to 2001. We assumed that fertilization increased linearly from 1895 to 1945 and used the average increase rate of the late 1940s to estimate the amounts of nitrogen fertilizer between 1895 and 1945. We further assumed that nitrogen fertilization application remained unchanged from 2001 to 2007.

Historical annual CO_2 concentration: In this simulation, standard IPCC historical CO_2 concentration data (Enting et al., 1994) was used for years before 2003. Annual CO_2 concentration data for years after 2003 were from Earth System Research Laboratory (ESRL, http://www.esrl.noaa.gov/gmd/ccgg/trends/).

Soil properties: We obtained the spatial maps for soil bulk density and soil pH of the study region from the 1 km × 1 km resolution digital general soil association map (STATSGO map) developed by the United States Department of Agriculture (USDA) Natural Resources Conservation. The soil textures, represented by the volumetric percentage of clay, sand, and silt, were estimated using the USDA soil texture triangle (Miller and White, 1998).

Topography map: The basic topographic information including elevation, slope, and aspect were derived from the 7.5 min USGS National Elevation Dataset (http://edcnts12.cr.usgs.gov/ned/ned.html).

Climate data: In this study we reconstructed a 8 km × 8 km resolution daily climate dataset of the entire SUS region from 1895 to 2007 by integrating the daily climate patterns of the North American Regional Reanalysis (NARR) dataset (http://wwwt.emc.ncep.noaa.gov/mmb/rreanl/) that covers the period of 1979–2005 into the monthly climate dataset (1895–2007) developed by PRISM (Parameter-elevation Regressions on Independent Slopes Model) Group at Oregon State University (http://prism.oregonstate.edu/).

Furthermore, we generated a 30-year detrended climate dataset (1895–1924) from the interpolated climate dataset (1961–1990) for model spinning run after equilibrium which could avoid sudden vibrations in model results due to simulation mode changes from equilibrium mode to transient mode.

Nitrogen deposition data: Nitrogen deposition datasets (NH_x-N and N_xO_y-N) were reconstructed based on the three time period (1860, 1993, and 2050) global nitrogen deposition dataset developed by Dentener (2006) and the decadal global anthropogenic trace gas emission datasets developed by Van Aardenne et al. (2001). The anthropogenic emission datasets were used to interpolate the annual data among the three time periods based on the assumption that the long-term variations of atmospheric nitrogen deposition were positively correlated with anthropogenic trace gas emissions.

Tropospheric ozone exposure data: AOT40 was used as an index of ozone damage on terrestrial ecosystems. The AOT40 dataset between 1941 and 1995 was derived from the global historical AOT40 datasets (at one-half degree resolution) developed by Felzer et al. (2005). These datasets were produced by combining the results from MATCH model (Multiscale Atmospheric Transport and Chemistry) and MIT IGSM (Integrated Global Systems Model). More details on these datasets can be found in Ren et al. (2007a,b). The dataset developed by Felzer et al. ended in 1995. Based on the annual mean ozone concentration records from the database of Clean Air Status and Trends Network (http://www.epa.gov/astnet/), we found that observed tropospheric ozone concentration did not vary significantly in the SUS after 1995. Therefore, we used the mean AOT40 values of the early 1990s to represent the values during 1995–2007.

All of the above datasets were generated based on existing spatial and temporal datasets or on historical inventory data.

Table 1
Comparison of model-simulated with field-observed annual GPP ($g\ C/m^2/yr$) and ET (mm).

Site	Measured GPP*	Simulated GPP	Measured ET*	Simulated ET	Time period	
Duke Hardwood Forest (US-DK2, NC, USA)	1650	1759	671.9	635	2003	AmeriFlux site
	1745	1786	576.7	611	2004	
	1716	1794	544.5	611	2005	
Duke Loblolly Pine Forest (US-DK3, NC)	1954	1851	599.7	600	2003	AmeriFlux site
	2175	2006	591.3	595	2004	
	2584	2044	579.5	603	2005	
Parker Track Loblolly Pine (NC, USA)	2519	2354	1024	890	2005	Noormets et al. (2009); Sun et al. (this issue)
Grassland (US-Shd, OK, USA)			589	661	1998	AmeriFlux site
			638	643	1999	
Fermi Prairie (US-IB2, IL, USA)	1308	1238			2005	AmeriFlux site
	1263	1244			2006	
	1383	1251			2007	
Cropland (US-ARM, OK, USA)	663	495	473	433	2004	AmeriFlux site
	532	536			2005	
	495	662	440	545	2006	

* The measured GPP and ET data from AmeriFlux sites have some missing data in some years.

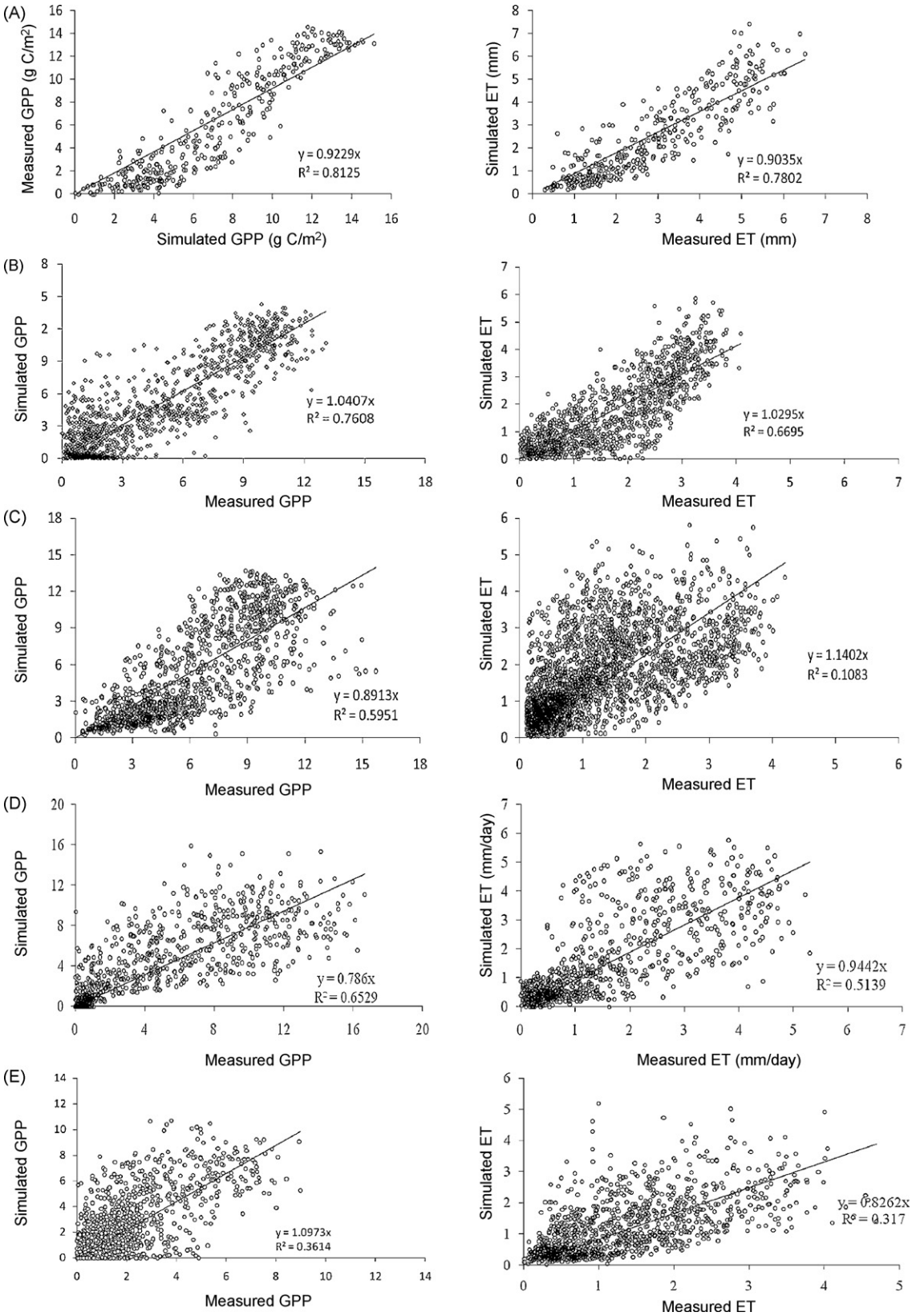

Fig. 5. Evaluation of model-simulated against field-measured daily GPP (g C/m^2/day) and ET (mm/day) at sites: (A) North Carolina Loblolly Pine (US-NC2, evergreen needleleaf forest) in 2005; (B) Duke Forest Hardwoods (US-DK2, NC, USA, deciduous broadleaf forest) from 2003 to 2005; (C) Duke Forest Loblolly Pine (US-DK3, evergreen needleleaf forest) from 2003 to 2005; (D) Shidler Tallgrass Prairie (US-shd, OK, USA, C_4 grassland) from 1998 to 1999; (E) ARM SGP Main (US-arm, OK, USA, cropland) from 2003 to 2006.

The temporal and spatial patterns and change rates of climate (precipitation and air temperature), tropospheric ozone concentration, nitrogen deposition, and land-use and land-cover types in the SUS are shown in Figs. 3 and 4, respectively.

2.4. Simulation experiments and methods

To address the effects of changing climate and combined environmental factors in this study, we designed two simulation experiments: (1) Climate change only (CLM): only climate changes with time and other environmental factors stay constant during the study period. The land-use and land-cover types, atmospheric CO_2 concentration and nitrogen deposition level in 1895 were used as input data and do not change over time; (2) Combined scenario (COMB): all the environmental factors change over time.

DLEM was first run to an equilibrium state using the mean climate data (averaged from 1961 to 1990) to develop the simulation baseline for carbon, nitrogen, and water pools. Then a 90-year spin-up simulation was conducted to eliminate system fluctuations caused by simulation mode shift, i.e., from the equilibrium mode to the transient mode.

2.5. Model calibration and evaluation

The DLEM has been parameterized and applied in several regional studies both in China and the United States using various field observational data for all defined plant functional types (Fig. 2), and then validated with independent field observational data, inventory data and regional estimations from other models and remote sensing tools (Chen et al., 2006a,b; Ren et al., 2007a,b; Zhang et al., 2007; Tian et al., 2008, submitted for publication). Specifically, the model was recalibrated for all the plant functional types except build-up land in SUS. These plant functional types included: temperate deciduous broadleaf forest, temperate evergreen needleleaf forest, mixed needleleaf and broadleaf forest, deciduous shrubland, C_3 grassland, C_4 grassland, grass wetland, forest wetland, and cropland (Fig. 2). The selected calibration sites were located in or close to the southern United States: Duke Forest, NC (36.0°N, −79.1°W, temperate evergreen needleleaf forest), Coweeta Long Term Ecological Research (LTER), NC (35.0°N, −83.5°W, temperate deciduous broadleaf forest), Florida Coastal Everglades, FL (25.47°N, −80.85°W, C_3 grassland), Konza Prairie LTER, KS (39.09°N, −96.58°W, C_4 grassland), Jornada Basin LTER, NM (32.62°N, −106.74°W, desert shrubland), a forest wetland in FL (25.24°N, −80.62°W, temperate evergreen needleleaf forest), and croplands with cotton, wheat, corn and soy bean (average soil carbon and NPP for different crop types from Oak Ridge National Laboratory were used for calibration).

We evaluated the simulated results for GPP and ET against those from several sites in the SUS as shown in Table 1 and Fig. 5. Generally, the simulated GPP and ET by DLEM fit well with the measured daily GPP and ET data, although there were many uncertainties, especially in the estimation of ET (Table 1 and Fig. 5). We also evaluated the simulated aboveground NPP at the regional scale using 138 field-observation data obtained from ORNL (Zheng et al., 2003). These observation data came from different plant functional types including forest, cropland, grassland and shrubland. The fitted line between measured aboveground NPP (X) and simulated aboveground NPP (Y) was: $Y = 1.09X + 73$, with a relatively high correlation coefficient ($R^2 = 0.82$). The DLEM estimated carbon storage for different carbon pools and evaluated different states in the SUS (see Tian et al., submitted for publication).

3. Results and analyses

3.1. Temporal and spatial variability of net primary productivity

In this study, changes in five environmental factors (climate, atmospheric ozone concentration and nitrogen deposition, CO_2 concentration and land-use types) were all combined (COMB) in our model simulation, which revealed the overall response of terrestrial ecosystems to environmental changes. During 1895–2007, we found that annual mean NPP of the terrestrial ecosystems in the SUS was 1.18 Pg C/yr and ranged from 0.92 Pg C/yr in 1925 to 1.45 Pg C/yr in 2001 (Fig. 6A). Although it varied substantially across the years, the NPP of terrestrial ecosystems in the SUS showed a tendency to increase from 1895 to 2007. NPP increased from about 1.05 Pg C/yr (463 g C/m^2/yr) to 1.33 Pg C/yr (587 g C/m^2/yr) with an increase rate of 27% (2.5 Tg C/yr) during the study period.

We found substantial regional variation in the annual NPP of terrestrial ecosystems in the SUS (Fig. 7A). Higher NPP was located in the eastern part of the SUS, while the lowest NPP was

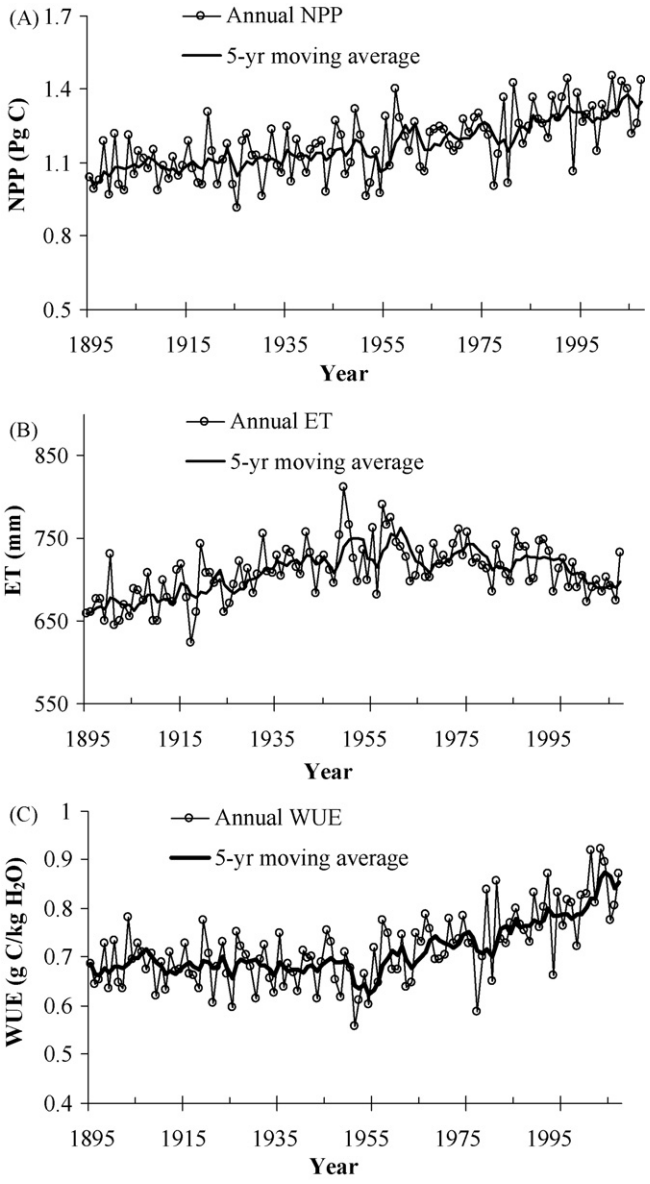

Fig. 6. Annual NPP (Pg C/yr), ET (mm) and WUE (g C/kg H_2O) across the terrestrial ecosystems of the southern United States during 1895–2007.

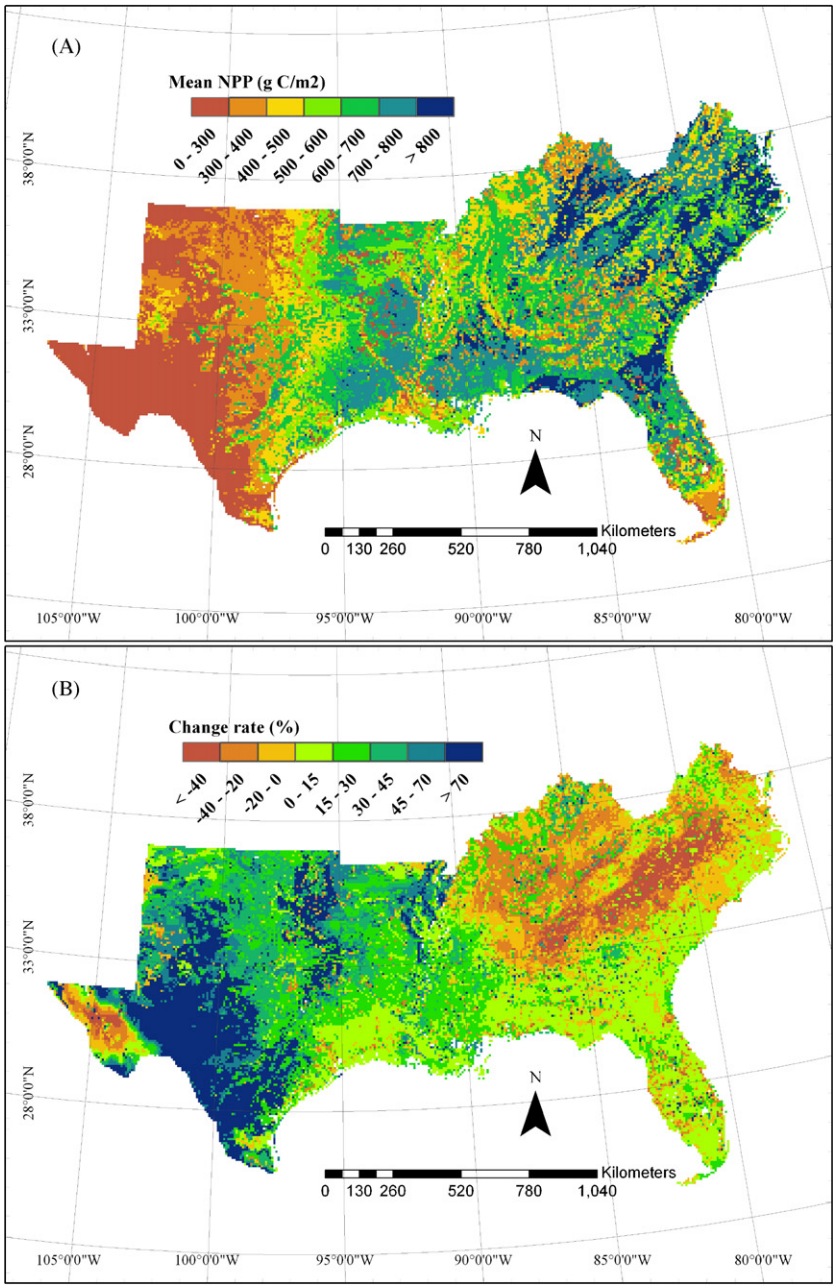

Fig. 7. Spatial distribution of annual mean NPP across the terrestrial ecosystems of the southern United States during 1895–2007 (g C/m^2/yr, A) and NPP change rate (%, B) from 1961–1990 to 1991–2007.

in the western part. Water is one of the most limiting factors affecting plant growth in the SUS; consequently, the general pattern of NPP for a specific ecosystem of natural vegetation types is similar to the precipitation distribution pattern (Fig. 4B). Uneven changes in environmental factors make the responses of NPP to environmental change different across the SUS. Although NPP generally increased from the period 1960–1990 to 1991–2007 (Fig. 7B), it decreased in some areas where land was converted from a higher to a lower productivity (e.g., from natural vegetation to urban area) as well as in the northeastern part of the region where drought events were frequent during 1991–2007 (Fig. 4C). The greatest increase (>70%) in NPP was in the shrubland region of the western part of the SUS and was attributed to a higher increase rate in precipitation in this region (Fig. 4C).

3.2. Temporal and spatial variability of evapotranspiration

The averaged overall annual ET at the regional scale did not change much over the entire period. Annual ET values ranged from a low of 624 mm in 1917 to a high of 812 mm in 1949 with an average of 710 mm from 1895 to 2007 (Fig. 6B). ET had an increasing trend during the first half of the period (1895–1950s), but a decreasing trend after that. The overall increase was negligible during the entire study period. Generally, the ratio of annual ET to precipitation was around 0.67, which means that about 33% of the rainfall was not used by the ecosystems if we disregard water used for cropland irrigation.

ET showed great spatial variability across the SUS (Fig. 8A). The highest ET was generally found in the grass and forested wetlands, as well as irrigated croplands. The lowest ET was found

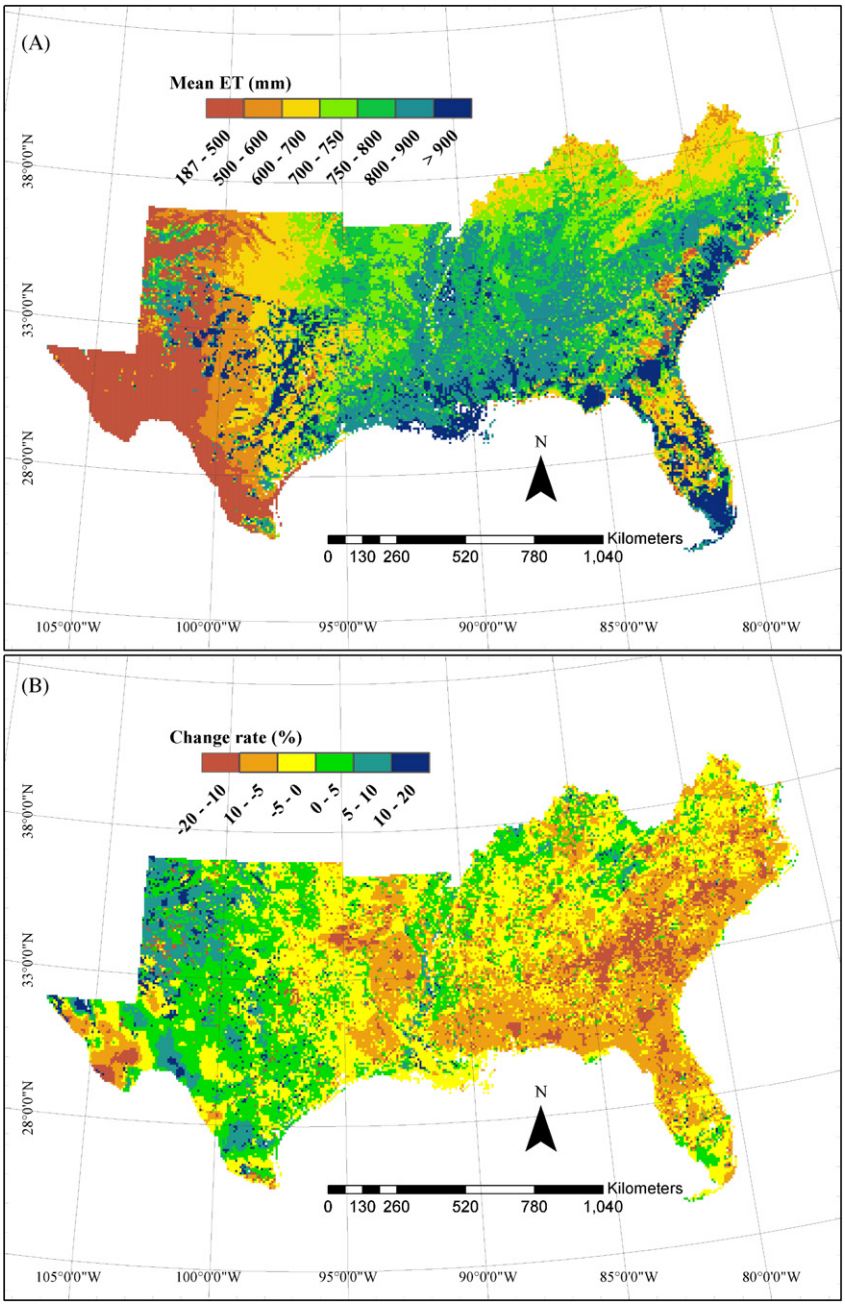

Fig. 8. Spatial distribution of annual mean ET across the terrestrial ecosystems of the southern United States during 1895–2007 (mm, A) and ET change rate (%, B) from 1961–1990 to 1991–2007.

in the shrubland in the western part of the SUS. ET decreased from 1961–1990 to 1991–2007 in the southeastern and central parts of SUS, and increased in the western SUS (Fig. 8B). Although precipitation in most areas of the southeastern SUS increased (Fig. 4C), ET decreased from 1961–1990 to 1991–2007. This implies that the change rate of ET might not be consistent with that of precipitation, and other factors such as land-use and land-cover change may play a role in the hydrologic balance. The highest ET/PPT (i.e., ET/precipitation) ratio was found in the driest region (Fig. 9), which implies that a higher percentage of precipitated water was used by land ecosystems in the driest regions. The reason for this high ET/PPT ratio is probably the higher potential demand for water and the lower amount of precipitation available.

3.3. Temporal and spatial variability of water use efficiency

WUE of the plants in the terrestrial ecosystems of the SUS ranged from 0.56 g C/kg H_2O in 1951 to 0.92 g C/kg H_2O in 2003 with an average of 0.71 g C/kg H_2O during 1895–2007 (Fig. 6C), which implied that about 0.71 g C had been fixed in the plants as net primary productivity by using 1 kg water. WUE was relatively stable before the 1950s and then increased after that with a substantial inter-annual fluctuation. WUE totally increased about 25% during 1895–2007.

The highest WUE (1.0–1.3 g C/kg H_2O) was in the eastern SUS (Fig. 10A), while the lowest WUE was in the western SUS. Although a higher ET/PPT ratio was found in the western SUS, WUE was significantly lower than that in the regions with higher

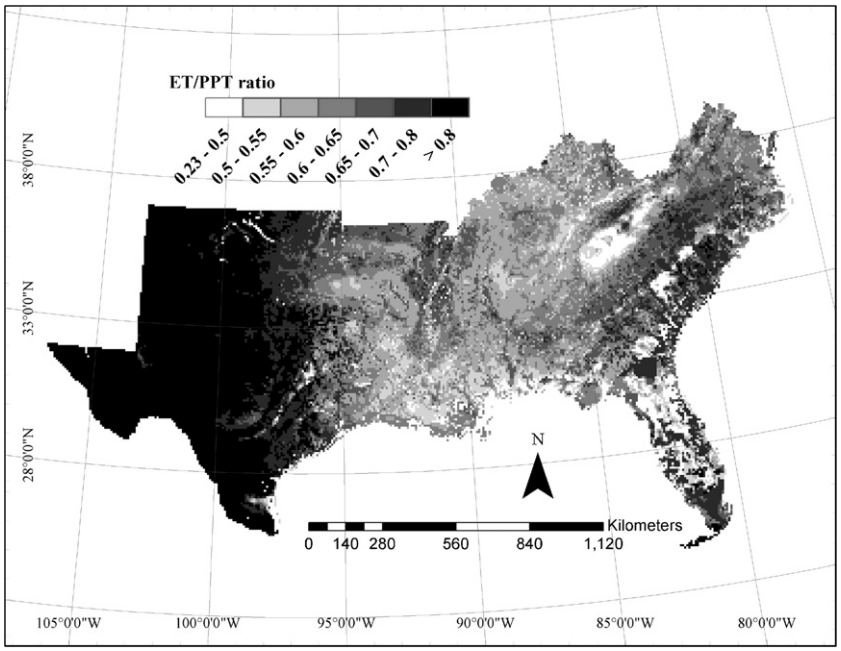

Fig. 9. Mean evapotranspiration/precipitation (ET/ppt) ratio across the terrestrial ecosystems of the southern United States during 1895–2007.

precipitation (Fig. 4B). WUE increased in most areas of the SUS from 1961–1990 to 1991–2007 with the highest increase in the southwestern SUS (Fig. 10B).

3.4. Different responses of NPP, ET and WUE among biomes

Different biomes respond differently to environmental changes in the SUS. NPP (g C/m^2/yr) of all the biomes has increased from 1895–1950 to 1951–2007, with the largest increase in cropland (about 41%, Table 2). Although cropland area decreased after the 1940s (Fig. 3E), the total NPP (Pg C/yr) of cropland in the SUS still increased the most (about 15%) compared to other biomes during 1951–2007. In addition, NPP of grassland and shrubland has increased about 15%, second to that of cropland. Area-averaged NPP for all the biomes in the entire SUS increased about 12% during 1895–2007.

ET of all the biomes except for temperate evergreen needleleaf and deciduous broadleaf forest increased from 1895–1950 to 1951–2007. ET of cropland increased about 9.4% under multiple environmental changes, while other biomes only slightly increased. Due to the different change rates of biome areas, the total ET increased slightly (about 2%) for all biomes as a whole.

The temperate evergreen needleleaf forest had the highest WUE (0.96 g C/kg H_2O), while shrubland had the lowest (0.45 g C/kg H_2O)

Table 2
Annual mean NPP, ET and WUE of different biomes in the southern United States.

Variables	PFT*	1895–1950	1951–2007	1895–2007
NPP (g C/m^2)	5	669 ± 24	679 ± 23	674 ± 16a**
	7	698 ± 12	715 ± 16	707 ± 10b
	11	220 ± 27	256 ± 28	239 ± 20c
	13	310 ± 14	355 ± 13	333 ± 10d
	15	660 ± 5	676 ± 8	668 ± 5a
	23	369 ± 3	520 ± 20	445 ± 17e
ET (mm)	5	743 ± 10	740 ± 8	742 ± 6a
	7	735 ± 10	736 ± 14	735 ± 8b
	11	450 ± 22	467 ± 21	458 ± 15c
	13	550 ± 18	586 ± 16	568 ± 13d
	15	891 ± 9	902 ± 12	897 ± 8e
	23	781 ± 8	855 ± 6	818 ± 8f
WUE (g C/kg H_2O)	5	0.90 ± 0.02	0.92 ± 0.03	0.91 ± 0.02a
	7	0.95 ± 0.01	0.97 ± 0.03	0.96 ± 0.01b
	11	0.42 ± 0.03	0.49 ± 0.04	0.45 ± 0.02c
	13	0.56 ± 0.01	0.61 ± 0.01	0.58 ± 0.01d
	15	0.75 ± 0.01	0.75 ± 0.01	0.75 ± 0.01e
	23	0.47 ± 0.00	0.61 ± 0.02	0.54 ± 0.02f
Area-averaged NPP		495	554	525
Area-averaged ET		699	721	710
Area-averaged WUE		0.68	0.75	0.72

* PFT5: Temperate deciduous broadleaf forest; PFT7: temperate evergreen needleleaf forest (including mixed forest); PFT11: deciduous shrubland; PFT13: C_3 and C_4 grassland; PFT15: grass and forest wetland; PFT23: cropland.

** Mean ± 2S.E. (2 standard error, 95% confidence interval). Different letters among groups mean significant difference at $P < 0.05$.

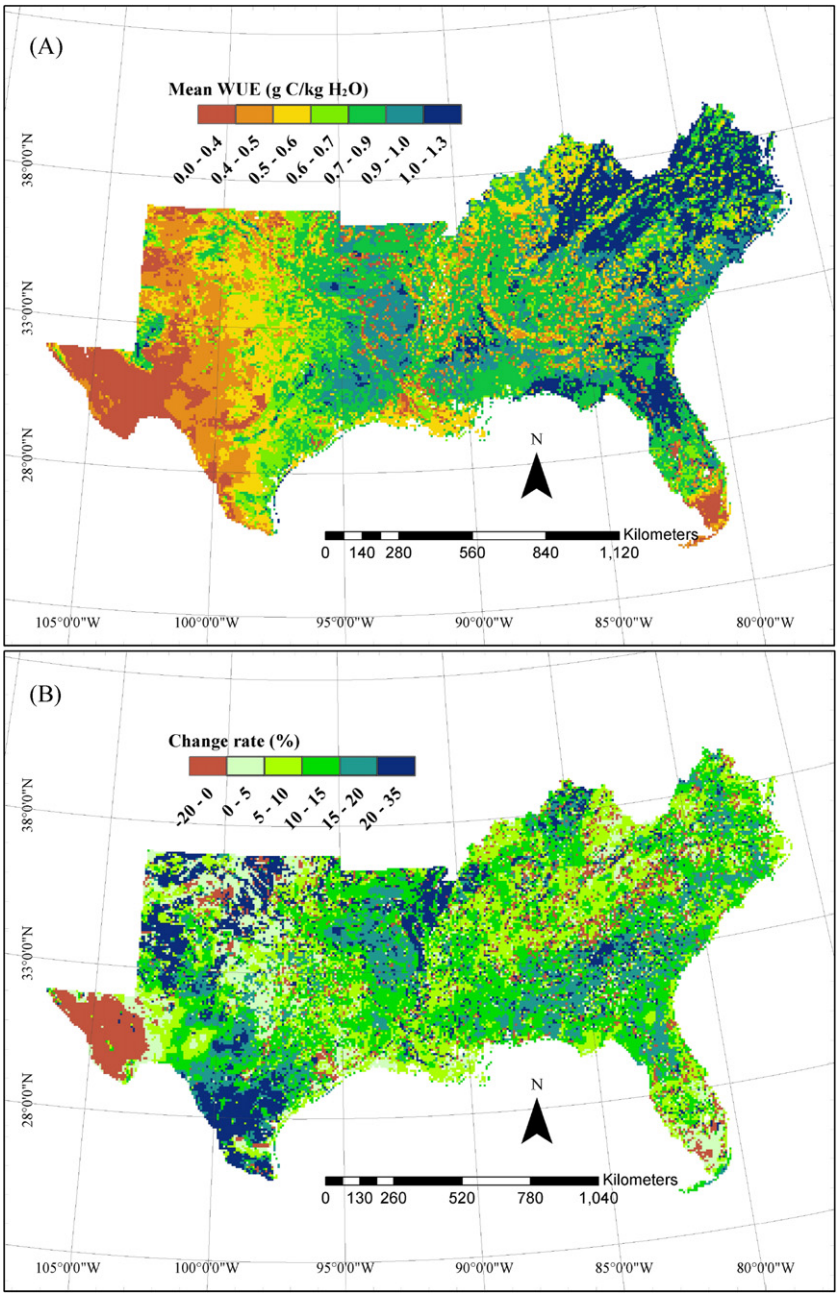

Fig. 10. Spatial distribution of mean annual WUE across the terrestrial ecosystems of the southern United States during 1895–2007 (g C/kg H_2O, A) and change rate (%, B) from 1961–1990 to 1991–2007.

among all biomes. Because large areas of croplands in the SUS were irrigated, the ET of cropland was much higher than that of grassland. Therefore, the WUE of cropland is lower than that of grassland though NPP of cropland (445 g C/m^2/yr) is significantly higher than that of grassland (333 g C/m^2/yr). WUE can be both impacted by NPP and ET, so the changing patterns of WUE for different biomes are different from those of NPP and ET during 1895–2007. WUE of forest and wetland did not change greatly under multiple environmental changes. Generally, forest and wetland are relatively water-abundant ecosystems (Webb et al., 1978), so WUE of these two biomes is not significantly affected by multiple environmental changes. In contrast, grassland, shrubland and most cropland are generally water-limited ecosystems. The WUE of grassland, shrubland and cropland increased about 9%, 17%, and 30%, respectively from 1895–1950 to 1951–2007.

3.5. Impacts of climate change on water use efficiency

Environmental changes such as changes in climate, atmospheric CO_2 concentration and nitrogen deposition, tropospheric ozone and land-use and land-cover types have been reported to influence WUE. WUE was reported to change with precipitation (Huxman et al., 2004; Emmerich, 2007; McLaughlin et al., 2007). In this study, the model simulation results from the climate only scenario (CLM) also indicated that WUE of different biomes responded differently to the precipitation gradient in the SUS. WUE of temperate deciduous broadleaf forest slightly decreased with an increase in precipitation (Fig. 11A). However, the WUE of the evergreen needleleaf forest first increased and then remained relatively stable with increasing precipitation (Fig. 11B). This can be explained by NPP increasing faster than ET with an increase in

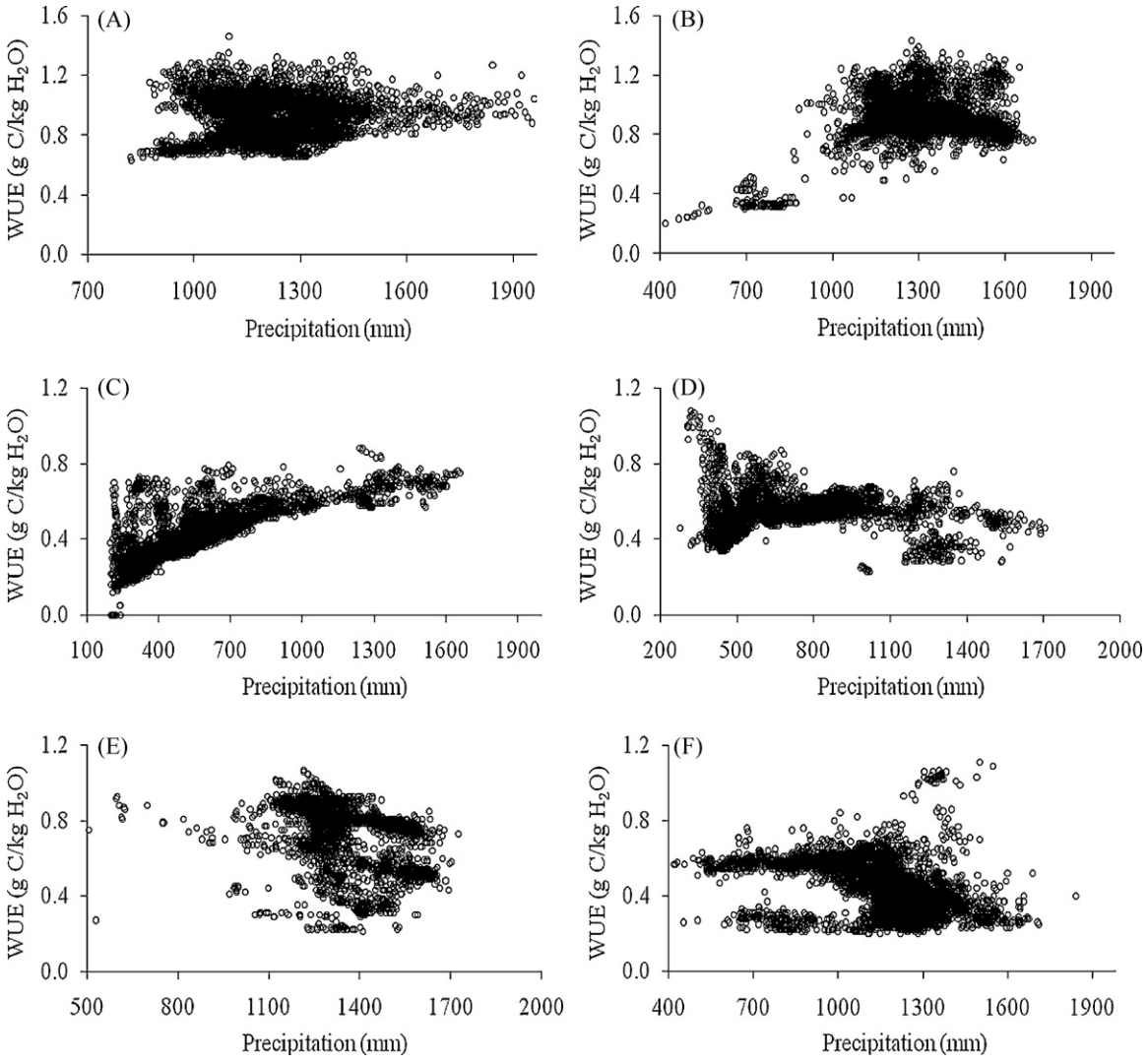

Fig. 11. Relationships between precipitation and water use efficiency for different biomes in the southern United States (A: temperate deciduous broadleaf forest; B: temperate evergreen needleleaf forest; C: shrubland; D: grassland; E: wetland; F: cropland).

precipitation in the regions of lower precipitation, while ET increased much faster than NPP in the regions of relatively higher precipitation. WUE of shrubland always showed an increasing trend with precipitation (Fig. 11C). WUE of grassland increased in the regions of lower precipitation and then stabilized (Fig. 11D). WUE of wetland ecosystems that were not water-limited decreased with increasing precipitation, suggesting little change in NPP over time (Fig. 11E). WUE of cropland did not show an obvious pattern with increasing precipitation due to the compound effects of irrigation (Fig. 11F).

4. Discussion

4.1. Water use efficiency of different biomes

Different water use efficiencies have been found among different plant species (Huxman et al., 2004; Ponton et al., 2006; Emmerich, 2007; Yu et al., 2008). In this study, we found that the WUE of different biomes showed a decreasing order of: Forest > Wetland > Grassland > Cropland > Shrubland in the southern United States. Using a different WUE definition from this study, Emmerich (2007) also found that ecosystem WUE (i.e., net ecosystem production/ET) of grassland is higher than that of shrubland in Arizona, U.S.A. Eddy covariance systems provided a good way to study carbon and water fluxes and thus WUE at a field level. Based on the synthesis data from FLUXNET, Law et al. (2002) has also calculated WUE for different biomes around the world and found that monthly WUE for several major biomes was similar, with the exception of arctic tundra, which was lower. However, by reselecting the sites located in the United States from Law et al. and assuming NPP/GPP ratio as 0.45, we found that the average annual WUE for temperate deciduous broadleaf forest was 1.12 g C/kg H_2O, evergreen needleleaf forest was 1.08 g C/kg H_2O, grassland was 0.94 g C/kg H_2O and cropland was 0.89 g C/kg H_2O. Our study showed the same pattern as reported by Law et al. (2002) that WUE of forests is higher than grassland and the lowest is found in cropland. However, the modeled regional absolute values of WUE derived from this study (Table 2) were lower than those reported by Law et al. (2002).

4.2. Drought impacts on NPP, ET and WUE

In this study, the distribution patterns of NPP, ET and WUE were found to closely relate to temporal and spatial precipitation patterns. Several severe drought events were reported in recent years (2001–2002, 2007–2008). The precipitation at the

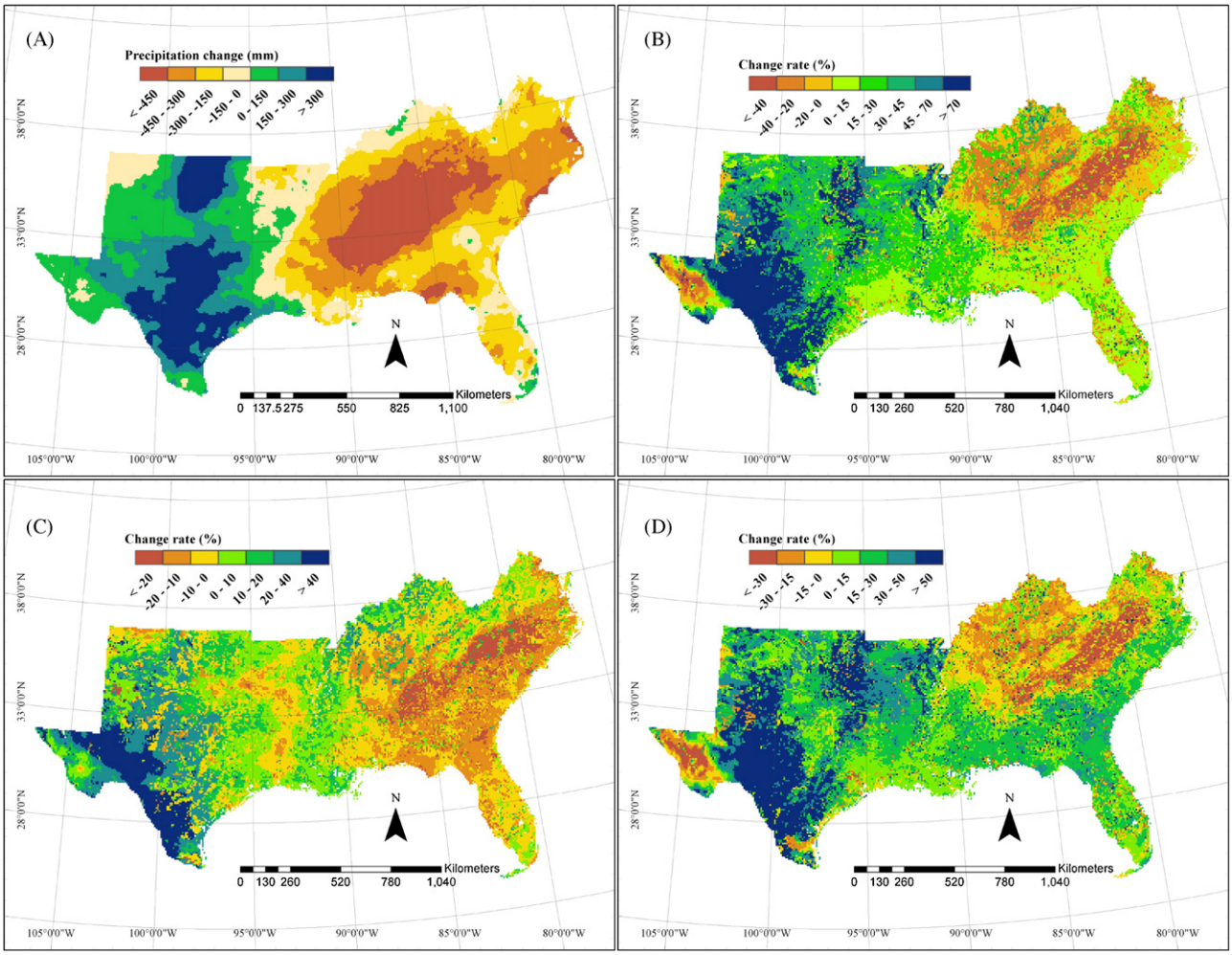

Fig. 12. Precipitation (mm, A), and NPP (g C/m^2/yr, B), ET (mm, C) and WUE (g C/kg H_2O, D) anomalies (relative to 1961–1990 mean) in 2007 in the southern United States.

northeastern part of SUS in 2007 was much lower than the mean values during 1961–1990, while precipitation was higher than normal in the central and western parts of SUS (Fig. 12). Although precipitation was reduced throughout the eastern SUS (Fig. 12A), NPP in 2007 still increased in areas where precipitation slightly decreased (Fig. 12B). This might imply that precipitation was not a dominant limiting factor to NPP in 2007 and the vegetation in this region has a buffering capability to tolerate drought events. A study on a loblolly pine (*Pinus taeda* L.) plantation in the lower coastal plain also suggested the 2007 drought did not affect NPP as most literature would suggest (Noormets et al., 2009). ET in 2007 decreased in most of the drought areas with a maximum reduction over 20% (Fig. 12C). The 20% reduction of ET may be caused by reduction of canopy interception rather than by plant transpiration as a recent study suggested (Sun et al., this issue). ET still increased in some areas of irrigated cropland and wetland even when precipitation greatly decreased. The changing spatial pattern of WUE is similar to that of NPP, displaying a great decrease in extreme drought areas (Fig. 12D). The underlying mechanisms of different ecosystems' response to changing environmental factors need to be specifically examined.

4.3. Implications to management and policy makers

Scaling up ecosystem processes from the field level, where most empirical data are derived, to the regional scale remains a challenge in global change studies (Tian et al., 2003, 2008; Waring and Running, 2007). Land managers and policy makers demand comprehensive, large-scale data for evaluating the range of changing environments and selecting rational management options. Our study found that annual precipitation in the SUS varied greatly. Even in the regions of high precipitation such as in North Carolina, drought is still one of the major threats to ecosystem productivity and health. Common management goals in the SUS are to preserve water, to maintain higher ecosystem productivity, and to maintain and promote healthy terrestrial ecosystems. In terms of ecosystem services, ecosystem water use and carbon sequestration often have conflicts in balancing carbon sequestration and water availability (Jackson et al., 2005). WUE reflects the tradeoffs between two important resources: water and carbon. We find that WUE of cropland is very low and will even be lower than our estimation if water losses through runoff after irrigation were considered in the calculation of WUE. Although we found that forest has a higher WUE, it was at the expense of large amounts of water to support its high productivity. SUS has a mild climate condition and large land area that can potentially be used for higher crop and forest production; therefore, bio-energy (e.g., biodiesel and ethanol) production has been encouraged in the SUS by the United States federal government. The land managers and policy makers have to consider the balance between productivity and water availability besides the efficiency of bio-energy production. Although there are many uncertainties in the model structure, model parameterization and input data, the spatial and

historical datasets and modeling results presented in this study may still help various agencies in developing their resource assessment and plans for mitigating and adapting to future energy demands and global change.

4.4. Uncertainties and future improvements

This study did not include irrigated water as part of the water used by crops in the calculation of WUE for cropland ecosystems. This simplification might result in an overestimation of WUE for croplands. Previous studies suggest that irrigation water should be quantified to accurately reflect the WUE of croplands (Hsiao, 1973; Howell, 2001). Although most of model input data are from available data sources which have been validated, there may still be many uncertainties in spatial and temporal interpolation of these data. Forest management (e.g., harvest and thinning) was not considered in this study, which might influence the results.

The model was parameterized with limited sites, so some uncertainties might also come from the model parameters. For example, canopy conductance, leaf water potential for full open/close stomatal conductance, and water vapor pressure deficit for full open/close stomatal conductance were parameterized as a constant for each plant functional type. The albedo for a specific plant functional type was also set as a constant within a simulation year. The uncertainties in model structure might have also compounded our simulation results to a certain degree. The simplification of some ecosystem processes in the model might not capture the exact patterns of real phenomena. Future improvements on these aspects of modeling will certainly reduce such uncertainties.

5. Conclusions

This study represents the first attempt to fully assess the long-term changes of NPP, ET, and WUE with the goal of understanding the interactions between carbon and water resources under multiple stresses at the regional scale in the southern U.S. Our results show that the NPP and WUE of terrestrial ecosystems have increased about 27%, and 25%, respectively, during 1895–2007 with substantial inter-annual variation, while ET has had little change as a whole. The increase in WUE was primarily stimulated by an increase in NPP, which was likely due to faster plant growth induced by environmental changes such as increasing CO_2 concentration and nitrogen deposition, and land management such as elevated irrigation and fertilizer usage. NPP, ET and WUE of various biomes were different and showed different responses to environmental changes. Substantial spatial variations of NPP, ET and WUE were found, which were associated with the spatial variations of multiple environmental factors during 1895–2007. Certainly, the contributions of different environmental factors to NPP, ET and WUE need to be further identified in future studies.

Acknowledgements

This study has been supported by the U.S. Department of Energy (DOE) NICCR Program, the USDA CSREES program and the Southern Forest Research Partnership (SFRP).

References

Agam, N., Berliner, P.R., Zangvil, A., Ben-Dor, E., 2004. Soil water evaporation during the dry season in an arid zone. Journal of Geophysical Research 109, D16103, doi:10.1029/2004JD004802.

Alexander, R.B., Smith, R.A., 1990. County-level estimates of nitrogen and phosphorus fertilizer use in the United States, 1945 to 1985: U.S. Geological Survey Open-File Report 90-130, 12 pp.

Bai, Y.F., Wu, J.G., Xing, Q., Pan, Q.M., Huang, J.H., Yang, D.L., Han, X.G., 2008. Primary production and rain use efficiency across a precipitation gradient on the Mongolia Plateau. Ecology 89, 2140–2153.

Birdsey, R.A., Heath, L.S., 1995. Carbon changes in U.S. forests. In: Joyce, L.A. (Ed.), Productivity of America's forests and climate change. Gen. Tech. Rep. RM-271. USDA Forest Service, Rocky Mountain Forest and Range Experiment Station, Fort Collins, CO, pp. 56–70.

Birdsey, R.A., Lewis, G.M., 2003. Current and historical trends in use, management, and disturbance of U.S. forestlands. In: Kimble, J.M., Heath, L.S., Birdsey, R.A., Lal, R. (Eds.), The Potential of U.S. Forest Soils to Sequester Carbon and Mitigate the Greenhouse Effect. CRC Press, New York, pp. 15–33.

Birdsey, R., Pregitzer, K., Lucier, A., 2006. Forest carbon management in the United States: 1600–2100. Journal of Environmental Quality 35, 1461–1469.

Bonan, G., 1996. The NCAR land surface model (LSM version 1.0) coupled to the NCAR community climate model. Technical Report NCAR/TN-429+STR. NCAR Boulder, Colorado.

Bray, E.A., 1997. Plant responses to water deficit. Trends in Plant Science 2, 48–54.

Chapin III, F.S., Matson, P.A., Mooney, H.A., 2002. Principles of Terrestrial Ecosystem Ecology. Springer Science, New York.

Chappelka, A.H., Samuelson, L.J., 1998. Ambient ozone effects on forest trees of the eastern United States: a review. New Phytologist 139, 91–108.

Chen, H., Tian, H., Liu, M., Melillo, J., Pan, S., Zhang, C., 2006a. Effect of land-cover change on terrestrial carbon dynamics in the southern USA. Journal of Environmental Quality 35, 1533–1547.

Chen, G., Tian, H., Liu, M., Ren, W., Zhang, C., Pan, S., 2006b. Climate impacts on China's terrestrial carbon cycle: an assessment with the dynamic land ecosystem model. In: Tian, H.Q. (Ed.), Environmental Modeling and Simulation. ACTA Press, pp. 56–70.

Collatz, G.J., Ball, J.T., Grivet, C., Berry, J.A., 1991. Physiological and environmental regulation of stomatal conductance, photosynthesis and transpiration: A model that includes a laminar boundary layer. Agricultural and Forest Meteorology 54, 107–136.

Collatz, G.J., Ribas-Carbo, M., Berry, J.A., 1992. A coupled photosynthesis- stomatal conductance model for leaves of C4 plants. Australian Journal of Plant Physiology 19, 519–538.

Dentener, F.J., 2006. Global Maps of Atmospheric Nitrogen Deposition, 1860, 1993, and 2050. Data set. Available on-line (http://daac.ornl.gov/) from Oak Ridge National Laboratory Distributed Active Archive Center, Oak Ridge, TN, U.S.A.

de Wit, C.T., 1958. Transpiration and crop yields. Agricultural Research Reports 64.6. Wageningen, Netherlands, Pudoc. 88 pp.

Dickinson, R.E., Henderson-Sellers, A., Kennedy, P.J., Wilson, M.F., 1993: Biosphere–atmosphere transfer scheme (BATS) version 1e as coupled for Community Climate Model. NCAR Tech. Note NCAR/TN-378+STR, 72 pp.

Donovan, L.A., Ehleringer, J.R., 1991. Ecophysiological differences among pre-reproductive and reproductive classes of several woody species. Oecologia 86, 594–597.

Eagleson, P.S., 1978. Climate, soil and vegetation, 2. The distribution of annual precipitation derived from observed storm sequences. Water Resources Research 14, 713–721.

Ehleringer, J.R., Buchmann, N., Flanagan, L.B., 2000. Carbon isotope ratios in belowground carbon cycle processes. Ecological Applications 10, 412–422.

Emmerich, W.E., 2007. Ecosystem water use efficiency in a semiarid shrubland and grassland community. Rangeland Ecology & Management 60, 464–470.

Entekhabi, D., Eagleson, P.S., 1989. Land surface hydrology parameterization for atmospheric general circulation models including subgrid scale variability. Journal of Climate 2, 816–831.

Enting, I.G., Wigley, T.M.L., Heimann, M., 1994. Future emissions and concentrations of carbon dioxide, key ocean/atmosphere/land analyses. CSIRO Division of Atmospheric Research Tech Paper No. 31. Melbourne.

Farquhar, G.D., von Caemmerer, S., Berry, J.A., 1980. A biochemical model of photosynthetic CO_2 assimilation in leaves of C_3 species. Planta 149, 78–90.

Farquhar, G., Sharkey, T., 1982. Stomatal conductance and photosynthesis. Annual Review of Plant Physiology 33, 317–345.

Felzer, B., Kicklighter, D., Melillo, J., Wang, C., Zhuang, Q., Prinn, R., 2004. Effects of ozone on net primary production and carbon sequestration in the conterminous United States using a biogeochemistry model. Tellus 56, 230–248.

Felzer, B., Reilly, J.M., Kicklighter, D., Sarofim, M., Wang, C., Prinn, R.G., Zhuang, Q., 2005. Future effects of ozone on carbon sequestration and climate change policy using a global biochemistry model. Climatic Change 73, 345–373.

Holland, E.A., Braswell, B.H., Sulzman, J.M., Lamarque, J.F., 2005. Nitrogen Deposition onto the United States and Western Europe. Data set. Available on-line (http://www.daac.ornl.gov) from Oak Ridge National Laboratory Distributed Active Archive Center, Oak Ridge, TN, U.S.A.

Homer, C., Huang, C., Yang, L., Wylie, B., Coan, M., 2004. Development of a 2001 National Landcover Database for the United States. Photogrammetric Engineering and Remote Sensing 70, 829–840.

Homer, C., Dewitz, J., Fry, J., Coan, M., Hossain, N., Larson, C., Herold, N., McKerrow, A., VanDriel, J.N., Wickham, J., 2007. Completion of the 2001 National Land Cover Database for the conterminous United States. Photogrammetric Engineering and Remote Sensing 73, 337–341.

Howell, T.A., 2001. Enhancing water use efficiency in irrigated agriculture. Agronomy Journal 93, 281–289.

Hsiao, T.C., 1973. Plant responses to water stress. Annual Review of Plant Physiology 24, 519–570.

Huxman, T.E., Smith, M.D., Fay, P.A., Knapp, A.K., Shaw, M.R., Loik, M.E., Smith, S.D., Tissue, D.T., Zak, J.C., Weltzin, J.F., Pockman, W.T., Sala, O.E., Haddad, B.M., Harte,

J., Koch, G.W., Schwinning, S., Small, E.G., Williams, D.G., 2004. Convergence across biomes to a common rain-use efficiency. Nature 429, 651–654.
IPCC, 2001. In: Houghton, J.T., Ding, Y., Griggs, D.J., Noguer, M., van der Linden, P.J., Dai, X., Maskell, K., Johnson, C.A. (Eds.), Climate Change 2001: The Scientific Basis. Cambridge University Press, Cambridge, UK, 881 pp.
IPCC, 2007. In: Solomon, S., Qin, D., Manning, M., Chen, Z., Marquis, M., Averyt, K.B., Tignor, M., Miller, H.L. (Eds.), Climate Change 2007: The Physical Science Basis, Contribution of Working Group I to the Fourth Assessment Report of the Intergovernmental Panel on Climate Change. Cambridge University Press, Cambridge, United Kingdom and New York, NY, USA, 996 pp.
Jackson, R.B., Jobbagy, E.G., Avissar, R., Roy, S.B., Barrett, D.J., Cook, C.W., Farley, K.A., le Maitre, D.C., McCarl, B.A., Murray, B.C., 2005. Trading water for carbon with biological carbon sequestration. Science 310, 1944–1947.
Jones, H.G., 1992. Plants and Microclimate: A Quantitative Approach to Environmental Plant Physiology. Cambridge University Press, Cambridge, UK.
Law, B.E., Falge, E., Gu, L., Baldocchi, D.D., Bakwin, P., Berbigie, P.R., Davis, K., Dolman, A.J., Falk, M., Fuentes, J.D., Goldstein, A., Granier, A., Grelle, A., Hollinger, D., Janssens, I.A., Jarvis, P., Jensen, N.O., Katul, G., Mahli, K., Matteucci, G., Myers, T., Monson, R., Munger, W., Oechel, W., Olson, R., Pilegaard, K., PawU, K.T., Thorgeirsson, H., Valentini, R., Verma, S., Vesala, T., Wilson, K., Wofsy, S., 2002. Environmental controls over carbon dioxide and water vapor exchange of terrestrial vegetation. Agricultural and Forest Meteorology 113, 97–120.
Lehner, B., Döll, P., 2004. Development and validation of a global database of lakes, reservoirs and wetlands. Journal of Hydrology 296, 1–22.
Liu, M., Tian, H., Zhang, C., Chen, G., Ren, W., Xu, X., Pan, S., Wang, X., Nagy, C., 2007. Effects of urbanization and land use on water yield—a case study of Haihe Basin in China. In: Proceedings of the Emerging Issues Along Urban/Rural Interfaces II: Linking Land-use Science and Society. pp. 90–96.
Liu, M., Tian, H.Q., Chen, G.S., Ren, W., Zhang, C., Liu, J., 2008. Effects of land use and land cover change on evapotranspiration and water yield in China during the 20th century. Journal of the American Water Resources Association (JAWRA) 44, 1193–1207, doi:10.1111/j.1752-1688.2008.00243.
Martin, M.J., Host, G.E., Lenz, K.E., 2001. Stimulating the growth response of aspen to elevated ozone: a mechanistic approach to scaling a leaf-level model of ozone effects on photosynthesis to a complex canopy architecture. Environmental Pollution 115, 425–436.
McLaughlin, S.B., Nosal, M., Wullschleger, S.D., Sun, G., 2007. Interactive effects of ozone and climate on tree growthand water use in a southern Appalachian forest in the USA. New Phytologist 174, 109–124.
McNulty, S.G., Vose, J.M., Swank, W.T., 1997. Regional hydrologic response of loblolly pine to air temperature and precipitation changes. Journal of the American Water Resources Association 33, 1011–1022.
Miller, D.A., White, R.A., 1998. A conterminous United States multi-layer soil characteristics data set for regional climate and hydrology modeling. Earth Interactions 2, (Online)In: http://EarthInteractions.org.
Nemani, R.R., Keeling, C.D., Hashimoto, H., Jolly, W.M., Piper, S.C., Tucker, C.J., Myneni, R.B., Running, S.W., 2003. Climate-driven increases in global terrestrial net primary production from 1982 to 1999. Science 300, 1560–1563.
NLCD, 2001. National Land Cover Database. U.S. Department of the Interior, U.S. Geological Survey. http://www.mrlc.gov/mrlc2k_nlcd.asp.
Noormets, A., Gavazzi, M., McNulty, S., Sun, G., Domec, J.C., King, J., Chen, J., 2009. Response of carbon fluxes to drought in a coastal plain loblolly pine forest. Global Change Biology, doi:10.1111/j.1365-2486.2009.01928.x.
Norby, R.J., DeLucia, E.H., Gielen, B., Calfapietra, C., Giardina, C.P., King, S.J., Ledford, J., McCarthy, H.R., Moore, D.J.P., Ceulemans, R., De Angelis, P., Finzi, A.C., Karnosky, D.F., Kubiske, M.E., Lukac, M., Pregitzer, K.S., Scarasci-Mugnozza, G.E., Schlesinger, W.H., Oren, R., 2005. Forest response to elevated CO_2 is conserved across a broad range of productivity. Proceedings of the National Academy of Sciences 102 , doi:10.1073/pnas.0509478102.
Ollinger, S.V., Aber, J.D., Reich, P.B., 1997. Simulating ozone effects on forest productivity: interactions among leaf-canopy and stand-level processes. Ecological Applications 7, 1237–1251.
Pereira, J.S., David, J.S., David, T.S., Caldeira, M.C., Chaves, M.M., 2004. Carbon and water fluxes in mediterranean-type ecosystems—constraints and adaptations. In: Esser, K., Luttge, U., Beyschlag, W., Murata, J. (Eds.), Progress in Botany, Springer-Verlag, Berlin Heidelberg, pp. 467–498.
Philip, J.R., 1957. The theory of infiltration. Sorptivity and algebraic infiltration. Soil Science 84, 257–264.
Ponton, S., Flanagan, L.B., Alstad, K.P., Johnson, B.G., Morgenstern, K., Kljun, N., Black, T.A., Barr, A.G., 2006. Comparison of ecosystem water-use efficiency among Douglas-fir forest, aspen forest and grassland using eddy covariance and carbon isotope techniques. Global Change Biology 12, 294–310.
Ren, W., Tian, H., Liu, M., Zhang, C., Chen, G., Pan, S., Felzer, B., Xu, X., 2007a. Effects of tropospheric ozone pollution on net primary productivity and carbon storage in terrestrial ecosystems of China. Journal of Geophysical Research 112, D22S09, doi:10.1029/2007JD008521.
Ren, W., Tian, H., Chen, G., Liu, M., Zhang, C., Chappelka, A., Pan, S., 2007b. Influence of ozone pollution and climate variability on grassland ecosystem productivity across China. Environmental Pollution 149, 327–335.
Ruddy, B.C., Lorenz, D.L., Mueller, D.K., 2006. County-level estimates of nutrient inputs to the land surface of the conterminous United States, 1982–2001. U.S. Geological Survey Scientific Investigations Report 2006-5012, accessed at http://pubs.usgs.gov/sir/2006/5012/.
Salinger, M.J., Sivakumar, M.V.K., Motha, R., 2005. Reducing vulnerability of agriculture and forestry to climate variability and change: workshop summary and recommendations. Climatic Change 70, 341–362.
Saxe, H., Cannell, M.G.R., Johnsen, B., Ryan, M.G., Vourlitis, G., 2001. Tree and forest functioning in response to global warming. New Phytologist 149, 369–399.
Sellers, P.J., Los, S.O., Tucker, C.J., Justice, C.O., Dazlich, D.A., Collatz, G.J., Randall, D.A., 1996. A revised land surface parameterization (SiB2) for atmospheric GCMs. Part I: Model formulation. Journal of Climate 9, 676–705.
Schimel, D., Melillo, J., Tian, H.Q., McGuire, D., Kicklighter, D., Kittel, T., Rosenbloom, N., Running, S., Thornton, P., Ojima, D., Parton, W., Kelly, R., Sykes, M., Neilson, R., Rizzo, B., 2000. Contribution of increasing CO_2 and climate to carbon storage by ecosystems in the United States. Science 287, 2004–2006.
Steduto, P., 1996. Water use efficiency. In: Pereira, L.S., Feddes, R.A., Gilley, J.R., Lesaffre, B. (Eds.),Sustainability of Irrigated Agriculture. NATO ASI Series E: Applied Sciences, Kluwer Academic Publishers, Dordrecht, pp. 193–209.
Still, C.J., Berry, J.A., Collatz, G.J., DeFries, R.S., 2003. Global distribution of C3 and C4 vegetation: carbon cycle implications. Global Biogeochemical Cycles 17, 1006, doi:10.1029/2001GB001807.
Sun, G., Amatya, D.M., Skaggs, R.W., Swift Jr., L.W., Shepard, J.P., Riekerk, H., 2002. A comparison of the watershed hydrology of coastal forested wetlands and the mountainous uplands in the Southern US. Journal of Hydrology 263, 92–104.
Sun, G., McNulty, S.G., Myers, J.A.M., Cohen, E.C., 2008. Impacts of multiple stresses on water demand and supply across the southeastern United States. Journal of the American Water Resource Association 44, 1441–1457.
Sun, G., Nooremets, A., Gavazzi, M.J., McNulty, S.G., Chen, J., Domec, J.C., King, J.S., Amatya, D.M., Skaggs, R.W., Energy and water balance of two contrasting Loblolly Pine Plantations on the lower coastal plain of North Carolina. Forest Ecology and Management, this issue, doi:10.1016/j.foreco.2009.09.016.
Tian, H.Q., Melillo, J.M., Kicklighter, D.W., Pan, S.F., Liu, J.Y., McGuire, A.D., Moore III, B., 2003. Regional carbon dynamics in monsoon Asia and its implications for the global carbon cycle. Global Planet Change 37, 201–217.
Tian, H.Q., Liu, M.L., Zhang, C., Ren, W., Chen, G.S., Xu, X.F., Lu, C.Q., 2005. DLEM—The Dynamic Land Ecosystem Model, User Manual. The EDGE Laboratory, Auburn University, AL, USA.
Tian, H.Q., Xu, X., Zhang, C., Ren, W., Chen, G., Liu, M., Lu, D., Pan, S., 2008. Forecasting and assessing the large-scale and long-term impacts of global environmental change on terrestrial ecosystems in the United States and China using an integrated regional modeling approach. In: Miao, S., Carstenn, S., Nungesser, M. (Eds.), Real World Ecology: Large-Scale and Long-Term Case Studies and Methods. Springer, New York.
Tian, H.Q., Zhang, C., Chen, G.S., Liu, M., Sun, G., Chappelka, A., Ren, W., Xu, X., Lu, C., Pan, S., Chen, H., Hui, D., McNulty, S., Lockaby, G., Vance, E., Patterns and controls of regional carbon budget in the Southern United States: response to multiple global change factors. submitted for publication.
Van Aardenne, J., Dentener, F., Olivier, J., Goldewijk, C.K., Lelieveld, J., 2001. A $1^\circ \times 1^\circ$ resolution data set of historical anthropogenic trace gas emissions for the period 1980–1990. Global Biogeochemical Cycles 15, 909–928.
Waisanen, P.J., Bliss, N.B., 2002. Changes in population and agricultural land in conterminous United States counties, 1790 to 1997. Global Biogeochemical Cycles 16, 1137.
Waring, R.H., Running, S.W., 2007. Forest Ecosystems Analysis at Multiple Scales, 3rd ed. Elsevier Academic Press, Burlington, San Diego, London.
Webb, W., Szarek, S., Lauenroth, W.K., Kinerson, R., Smith, M., 1978. Primary productivity and water use in native forest, grassland, and desert ecosystems. Ecology 59, 1239–1247.
Wigmosta, M.S., Vail, L.W., Lettenmaier, D.P., 1994. A distributed hydrology-vegetation model for complex terrain. Water Resources Research 30, 1665–1679.
Woodbury, P.B., Smith, J.E., Heath, L.S., 2007. Carbon sequestration in the U.S. forest sector from 1990 to 2010. Forest Ecology and Management 241, 14–27.
Wythers, K.R., Lauenroth, W.K., Paruelo, J.M., 1999. Bare-soil evaporation under semiarid field conditions. Soil Science Society of America Journal 63, 1341–1349.
Yu, G.R., Song, X., Wang, Q.F., Liu, Y.F., Guan, D.X., Yan, J.H., Sun, X.M., Zhang, L.M., Wen, X.F., 2008. Water-use efficiency of forest ecosystems in eastern China and its relations to climatic variables. New Phytologist 177, 927–937.
Zhang, C., Tian, H., Chappelka, A., Ren, W., Chen, H., Pan, S., Liu, M., Styers, D.M., Chen, G., Wang, Y., 2007. Impacts of climatic and atmospheric changes on carbon dynamics in the Great Smoky Mountains. Environmental Pollution 149, 336–347.
Zheng, D.L., Prince, S.D., Wright, R., 2003. NPP Multi-Biome: Gridded Estimates for Selected Regions Worldwide, 1989-2001i, R1. Data set. Available on-line (http://www.daac.ornl.gov) from the Oak Ridge National Laboratory Distributed Active Archive Center, Oak Ridge, TN, U.S.A.